

THEORETICAL RESEARCH PROGRAM  
TO STUDY CHEMICAL REACTIONS  
IN AOTV BOW SHOCK TUBES

Periodic Research Report  
Cooperative Agreement No. NCC2-371

for the period  
April 1, 1991 - December 31, 1991

Submitted to

National Aeronautics and Space Administration  
Ames Research Center  
Moffett Field, California 94035

Computational Chemistry Branch  
Dr. Stephen R. Langhoff  
Chief and Technical Monitor

Prepared by

ELORET INSTITUTE  
1178 Maraschino Drive  
Sunnyvale, CA 94087  
Phone: (408) 730-8422 and (415) 493 4710  
Telefax: (408) 730-1441  
K. Heinemann, President and Grant Administrator  
Peter Taylor, Principal Investigator

7 May, 1992

1279  
N93-11851  
--THRU--  
N93-11855  
Unclass

G3/72 0095585

(NASA-CR-188927) THEORETICAL  
RESEARCH PROGRAM TO STUDY CHEMICAL  
REACTIONS IN AOTV BOW SHOCK TUBES  
Periodic Research Report, 1 Apr. -  
31 Dec. 1991 (Eloret Corp.) 79 D

This report covers the period April 1 1991 to December 31 1991. Effort has continued through this period to refine and expand the SIRIUS/ABACUS program package for CASSCF and RASSCF second derivatives. One of the other authors of the package, Trygve Helgaker, and myself have devised a new approach to computing the Gaussian integral derivatives that require much of the time in gradient and Hessian calculations. This work has been written up and accepted for publication (copies attached).

Several different studies have been undertaken in the area of application calculations. These include a study of proton transfer in the HF trimer, which provides an analog of rearrangement reactions, and the extension of our previous work on Be and Mg clusters to Ca clusters. In addition, a very accurate investigation of the lowest-lying potential curves of the O<sub>2</sub> molecule was completed. These curves are essential for evaluating different models of the terrestrial atmosphere nightglow. All these studies have been written up and accepted for publication (copies attached).

We have recently repeated some of our earlier studies of the Ne atom hyperpolarizability, stimulated partly by concern about very small uncertainties in the perturbed energies because of SCF convergence difficulties, and partly by the publication of a RASSCF investigation that predicted a very different hyperpolarizability. By calibrating our earlier calculations against full CCSDT results we can be confident that our earlier result (corrected for the

convergence problems) should be much more reliable than the RASSCF result. This work has been written up and accepted for publication (copies attached).

Most effort this year has been devoted to a large-scale investigation of stationary points on the  $C_4H_4$  surface, and the thermochemistry and mechanisms of acetylene/acetylene reaction. Since acetylene is the last stable hydrocarbon species produced in the combustion of hydrocarbon fuels, it has been speculated that reaction between two  $C_2H_2$  species could be an important component of the overall combustion mechanism. Direct reaction of acetylene with itself to produce any  $C_4H_4$  products is likely to involve very high barriers; on the other hand, the very reactive vinylidene isomer of  $C_2H_2$  lies about 45 kcal/mol above acetylene. If significant quantities of vinylidene were formed these could react with acetylene to form a number of different  $C_4H_4$  isomers. In fact, the existence of numerous minima on the  $C_4H_4$  surface, including some forms well-described only at the MCSCF level and thus not previously characterized, has seriously complicated the investigation. However, it seems likely that all relevant minima have been found, and some effort has been invested in locating saddle points on various pathways (if indeed there are barriers). So far, it seems likely that vinylidene insertion into the acetylene CH bond will occur without a barrier, but there may be a barrier to CC bond insertion. This work is continuing.

# Theoretical study of the low-lying bound states of O<sub>2</sub>

Harry Partridge, Charles W. Bauschlicher, Jr. and Stephen R. Langhoff  
NASA Ames Research Center  
Moffett Field, CA 94035

Peter R. Taylor  
ELORET Institute†  
Palo Alto, CA 94303

## Abstract

*Ab initio* results are presented for the low-lying bound states of O<sub>2</sub> that dissociate to ground-state atoms. Spectroscopic constants and dissociation energies are reported for the  $X^3\Sigma_g^-$ ,  $a^1\Delta_g$ , and  $b^1\Sigma_g^+$ ,  $c^1\Sigma_u^-$ ,  $A'^3\Delta_u$ ,  $A^3\Sigma_u^+$ ,  $^3\Pi_u$ ,  $^5\Sigma_u^-$ ,  $^5\Pi_u$ , and  $^5\Pi_g$  states. For the six lowest states, which have been experimentally characterized, we obtain accurate results at the multireference configuration interaction plus Davidson correction level. For example, we compute a  $D_e$  value for the  $X^3\Sigma_g^-$  state to be only 1.5 kcal/mole less than the experimental result after we have corrected for basis set superposition error. The  $^5\Pi_g$  state is estimated to have a  $D_e$  of  $0.16\pm0.03$  eV, which suggests that the importance of this state in the nightglow should probably be reconsidered.

## I. Introduction

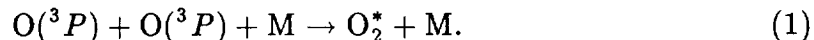
The six strongly bound states of O<sub>2</sub> that originate from ground-state atoms have been well characterized experimentally. More weakly bound states, such as  $^5\Pi_g$ , have not been observed and will be difficult to characterize experimentally. Yet a knowledge of the potential energy curves of these states is important for modelling a number of phenomena. For example, the potential energy curves for these states are required for the calculation of transport properties and for modelling the energy flow in the Earth's atmosphere.

The terrestrial atmosphere nightglow is known to have two components: the

---

† Mailing address: NASA Ames Research Center, Moffett Field, CA 94035

first is due to emission from the  $O_2\ a^1\Delta_g$  state, which is formed by the daytime photodissociation of  $O_3$ , and the second is due to emission from a series of excited states, which are formed by the recombination of O atoms. This second process is very complex and is not completely understood. The first step involves the formation of excited  $O_2$  molecules,



These excited molecules can radiate, react, relax collisionally, or dissociate. There seems to be general agreement that emission from several states, most notably  $b^1\Sigma_g^+$ , is more intense than can be explained solely by a direct population mechanism and that a precursor must be involved. Both collision



and reaction



are known to be important energy transfer mechanisms for  $O_2$ . For example, the reaction mechanism of eq. (3) is involved in the formation of  $O(^1S)$ , which is responsible for the nightglow green line.

Wraight [x] and Smith [x] calculated the atomic association rate (i.e., the rate of eq. (1)) into each of the bound states of  $O_2$  and suggested that at 200 K 70% of all associations took place into the  $^5\Pi_g$  state. The small  $D_e$  of the  $^5\Pi_g$  state leads to an increase in the dissociation rate state at higher temperatures, which results in a rapid fall off in O atom association rate at higher temperatures; their computed results were in good agreement with the experiments of Campbell and Gary. Hence Wraight suggested that the  $^5\Pi_g$  state might play a very important role as a precursor in the formation of  $O_2\ b^1\Sigma_g^+$  and  $O(^1S)$  in the Earth's atmosphere. To a large degree these conclusions were based on the  $^5\Pi_g$  potential energy curve calculated by Saxon and Liu, which has a  $D_e$  of 0.22 eV. Unfortunately, the first-order configuration-interaction (FOCI) method used by Saxon and Liu yields only qualitatively reliable binding energies, while the calculated association rates are quite sensitive to the  $D_e$  since the  $^5\Pi_g$  lifetime must be sufficiently long that it can be quenched to a more tightly bound state.

Using a smaller estimate for the  $D_e$ , Bates concluded that  $^5\Pi_g$  was not an important precursor for the formation of the more strongly bound states or in the production of  $O(^1S)$ . However, Bates suggested that it might play an important role in the formation of  $O_3$  in the lower atmosphere by the reaction



As these uncertainties in understanding the upper atmosphere are derived in part from the uncertainty in the dissociation energy of the  $^5\Pi_g$  state, we have undertaken a study to compute this quantity very accurately. In addition, there is little information about the other weakly bound states of  $O_2$ , such as  $^5\Sigma_u^-$ , which has been suggested as the state responsible for the perturbations in the  $A\ ^3\Sigma_u^+$  state. In this work we report on calculations on a number of the weakly bound valence states of  $O_2$ . The calculation of binding energies, in particular, for such systems is a challenging problem, and we have attempted to estimate the reliability of our calculations by examining the convergence of our results for the six strongly bound states characterized accurately by experiment. The computational requirements for obtaining reliable spectroscopic constants for these states should provide useful information on the requirements for describing the hitherto unobserved states. We demonstrate that a multireference configuration-interaction (MRCI) treatment with a Davidson correction (denoted +Q) in an extended basis set yields reliable results.

## II. Method

Most of the one-particle basis sets employed in this study are constructed using general contractions based on atomic natural orbitals (ANO) [1]. The first primitive set employed is that used in earlier work. The basis is derived from the  $(13s\ 8p)$  primitive set of van Duijneveldt supplemented with a  $(6d\ 4f\ 2g\ 1h)$  even-tempered set of polarization functions. The polarization functions are of the form  $\alpha = 2.5^n \alpha_0$  with  $n = 0 \dots k$  and  $\alpha_0 = 0.13, 0.39, 1.24$  and  $2.61$  for the  $d, f, g$ , and  $h$  functions, respectively. The geometric mean of the  $d$  exponents is derived from the optimum  $d$  exponent of Ahlrichs and Taylor. The primitive set was contracted to  $[6s\ 5p\ 4d\ 3f\ 2g\ 1h]$  based upon the natural orbitals obtained from atomic single and double excitation CI calculations correlating both the  $2s$

and  $2p$  electrons, and employing an occupation number selection criterion of  $10^{-5}$ . Smaller sets, such as the  $[5s\ 4p\ 3d\ 2f\ 1g]$  set, are obtained by deleting the shell of orbitals with the smallest occupation number. A second contracted set was derived by supplementing the contracted set with a diffuse  $s$  ( $\alpha = 0.076666$ ) and  $p$  ( $\alpha = 0.051556$ ) function and uncontracting the outermost  $d$  function giving a set designated  $[5s\ 4p\ 3 + 1d\ 2f\ 1g] + (sp)$ . Supplementing the basis with the diffuse functions improves the description of the oxygen atomic polarizability, an accurate description of which is necessary to calculate reliable interaction energies for weakly bound systems.

To investigate the convergence with respect to the primitive basis set, we employed an ANO set derived from a larger  $(18s\ 13p)$  primitive set. This set is quadruple zeta in the  $2s$  space and yields an atomic SCF energy only  $3\ \mu E_H$  above the numerical Hartree-Fock result. This primitive set is supplemented with a  $(6d\ 5f\ 4g)$  even-tempered set of polarization functions;  $\alpha_0 = 0.13, 0.25$ , and  $0.42$  for the  $d$ ,  $f$ , and  $g$  functions. The expanded  $f$  and  $g$  polarization sets are employed since work on Ne atom indicated that the smaller  $4f\ 2g$  sets might not be saturated. The primitive set was contracted to  $[5s\ 5p\ 3d\ 2f\ 1g]$  based upon the natural orbitals from atomic calculations: natural orbitals with occupation numbers greater than  $10^{-5}$  were selected. In addition, we employed the  $[9s\ 7p\ 4d\ 2f]$  segmented basis set from ref x. This set is a  $[7s\ 5p]$  contraction of the  $(13s\ 8p)$  set of Partridge supplemented with two diffuse  $s$ , two diffuse  $p$ , and a  $(4d\ 2f)$  polarization set. The basis set was derived for a study of the high-spin states of NO and at the coupled-pair functional (CPF) level gives an O atom polarizability of  $5.14\ a_0^3$ , or 95% of the recommended value. Only the pure spherical harmonic components of the  $d$ ,  $f$ ,  $g$ , and  $h$  functions are employed.

The orbitals were optimized using the complete-active space self-consistent-field (CASSCF) approach. While the calculations are performed in  $D_{2h}$  symmetry, full  $D_{\infty h}$  symmetry is imposed on the orbitals. In most cases the  $2p$  orbital and electrons are active. For the  $a^1\Delta_g$  and  $b^1\Sigma_g^+$  states, a state-averaged (SA) CASSCF approach is employed as they appear in the same  $D_{2h}$  irreducible representation. MRCI calculations correlating both the  $2s$  and  $2p$  electrons are performed: these include all single and double excitations from all configurations in CASSCF wave

function. The effect of higher excitations is estimated using a multireference analog of the Davidson correction, denoted +Q, and the size-extensive averaged coupled-pair functional (ACPF) method. Basis set superposition errors (BSSE) are estimated using the counterpoise method. All calculations were performed with the MOLECULE-SWEDEN program system.

### III. Results and Discussion

#### A. Strongly bound states

The calculated spectroscopic constants for the  $X^3\Sigma_g^-$ ,  $a^1\Delta_g$  and  $b^1\Sigma_g^+$  states in the different basis sets are compared with the experimental results in Table I. The  $r_e$  and  $\omega_e$  constants are derived from a fit in  $1/r$  to the theoretical results on a  $0.1 a_0$  grid. The  $D_e$  values are computed using a supermolecule to minimize size-consistency errors. Overall the results are in rather good agreement with experiment. For the ground state expanding the basis set from  $[4s\ 3p\ 2d\ 1f]$  to  $[5s\ 4p\ 3d\ 2f\ 1g]$  results in little change in  $r_e$  and  $\omega_e$ , but  $D_e$  is increased by almost 0.2 eV. Expansion to  $[6s\ 5p\ 4d\ 3f\ 2g\ 1h]$  has a much smaller effect, increasing  $D_e$  by about 0.05 eV. These results suggest that the calculated spectroscopic constants in our biggest basis set are near the basis set limit. Extending the  $[5s\ 4p\ 3d\ 2f\ 1g]$  basis set with diffuse functions (and uncontracting the outermost  $d$  primitive) increases the calculated  $D_e$  by about 0.025 eV, which is considerably more than the 0.009 eV obtained by substantially expanding the primitive basis set. Based on these results we use the  $[5s\ 4p\ 3 + 1d\ 2f\ 1g] + (sp)$  basis as our standard basis set in the remainder of this work. In this set the  $r_e$  and  $\omega_e$  values are in excellent agreement with experiment. At the MRCI level the calculated  $D_e$  values are about 0.15 eV less than the experimental results, whereas including the Davidson correction for higher excitations gives  $D_e$  values about 0.03 eV less than the experiment. This differs from previous work employing a  $[5s\ 4p\ 3d\ 2f\ 1g]$  ANO basis set, which suggested that the MRCI+Q level of treatment in these basis sets overestimated  $D_e$ . The discrepancy occurs since the highest  $\sigma_g$  and  $\sigma_u$  orbitals were deleted in the earlier work. At long range this corresponds to deleting a combination of the fourth and fifth  $s$  ANOs, while near  $r_e$  the orbitals are a combination of all possible  $\sigma$  components. Deleting these orbitals artificially raised the atomic asymptote (when



twelve electrons are correlated) resulting in a 0.08 eV overestimation of  $D_e$ . In comparisons with double zeta plus polarization basis eight-electron full CI calculations, the MRCI+Q treatment was shown to overestimate  $D_e$  by about as much as MRCI underestimates it. However, when  $2s$  correlation is included it is unlikely that the MRCI+Q treatment will significantly overestimate  $D_e$  and we consider the results at this level as the most reliable. In the ANO basis that includes  $h$  functions the MRCI+Q  $D_e$  value is slightly larger than experiment, but the difference is of the same order as the superposition error, as discussed below. The reliability of the Davidson correction is corroborated by the very similar results that are obtained at the ACPF level. Indeed, the ACPF results would suggest that the Davidson correction slightly underestimates the effect of higher excitations.

Compared with the  $X^3\Sigma_g^-$  MRCI results with eight electrons correlated of Ref. x, the effect of  $2s$  correlation is to reduce  $D_e$  by about 0.1 eV. This is considerably larger than the 0.04 eV reported earlier; as noted above the error in the older twelve-electrons correlated results arose from truncating the virtual orbital space. However, even this larger value is substantially less than the 0.3 eV reduction for  $N_2$ . The reduction in  $D_e$  in that case has been attributed to single excitations in the N atom from  $2s$  to  $3d$ , with a concomitant spin and symmetry recoupling of the  $2p$  electrons. In  $N_2$  this effect disappears at  $r_e$ , because all the  $2p$  electrons are coupled to a singlet to form the triple bond. The same atomic correlation effect arises in the O atom, but in the  $O_2$  ground state part of the effect persists even at  $r_e$ , because the  $2p$  electrons are not completely recoupled in forming the bond. Hence the reduction in  $D_e$  from  $2s$  correlation will be less in  $O_2$  than in  $N_2$ .

The basis set superposition errors, BSSE, for the different basis sets were estimated using the counterpoise method. At the MRCI+Q level the BSSE (per atom) at  $r=2.3 a_0$  is 0.022 eV for the  $[5s\ 4p\ 3d\ 2f\ 1g]$  and  $[5s\ 4p\ 3 + 1d\ 2f\ 1g] + (sp)$  basis set and 0.019 eV for the  $[5s\ 5p\ 3d\ 2f\ 1g]$  basis set. Most of the reduction in the BSSE is due to the improvement of the primitive polarization basis; expanding the  $s$  and  $p$  primitive spaces reduced the BSSE very slightly. Thus, corrected for BSSE the calculated  $D_e$  of the  $X^3\Sigma_g^-$  state is 0.063 eV (1.45 kcal/mole) smaller than the experimental  $D_e$ . We estimate that about half this error is due to basis set deficiencies, based on our experience with  $N_2$ . Core ( $1s$ ) correlation is likely to

contribute on the order of 0.7 kcal/mole.

In Table II, we compare the spectroscopic constants at the MRCI+Q level in the  $[5s\ 4p\ 3 + 1d\ 2f\ 1g] + (sp)$  basis set for the six bound states, dissociating to ground state atoms, that have been experimentally characterized. The calculated results are in excellent agreement for all of the states. Except for the  $a^1\Delta_g$  and  $b^1\Sigma_g^+$  states the calculated  $D_e$  are all within 0.025 eV of the experimental results. For the  $a^1\Delta_g$  and  $b^1\Sigma_g^+$  states the error is 0.053 and 0.041 eV, respectively. We have investigated the possibility that the use of SA-CASSCF orbitals is responsible for this, but the error from this source is only 0.01 eV. Overall, our results indicate that the computational procedure and basis set employed gives a good description of all of the low-lying states. In fact, the calculated potentials for the  $c^1\Sigma_u^-$ ,  $A'^3\Delta_u$ , and  $A^3\Sigma_u^+$  states, tabulated in Table III and plotted in Fig. 1, agree well with the RKR potentials, indicating that we are obtaining a good description for all  $r$  values.

## B. Weakly bound states

The computational requirements necessary to obtain an accurate description for weakly bound systems are severe, because the errors associated with the one- and  $n$ -particle space truncation can be of the same order of magnitude as the well depth. It is important that the computational procedure be able to describe the atomic polarizabilities well and to minimize the BSSE. The ANO basis sets employed in this work were contracted based upon a correlated treatment of the  $O(^3P)$  state. Thus, it is expected that, in some sense, these basis sets minimize the BSSE. In addition, by uncontracting or supplementing with diffuse functions, the basis sets permit an accurate description of the atomic properties.

For the weakly bound states of  $O_2$  dissociating to ground state  $O(^3P)$  atoms, the long range form of the potential is of the form

$$-V_{LR}(r) = \frac{C_5}{r^5} + \frac{C_6}{r^6} + \frac{C_8}{r^8} + \dots,$$

where the coefficient  $C_5$  arises from the quadrupole–quadrupole interactions,  $C_6$  is the dispersion coefficient arising from the induced dipole–induced dipole interaction, and  $C_8$  describes both dispersion and induction. We note parenthetically that the free O atom does not have a quadrupole moment, of course: it is only when the

atoms are perturbed, such as by another atom, that the degeneracy is lifted and it is meaningful to speak of the quadrupole moments of a specific configuration. In recent work on the high-spin states of NO we examined whether it is important to constrain the O atom at long range to be spherical, i.e., to ensure that all of the states dissociating to ground state atoms have the same asymptotic energy. We found that these constraints were not necessary for treatments that included correlation. In addition to substantially increasing the length of the CI expansion, the constraints reduced the reliability of the Davidson correction in the vicinity of the minimum. Thus the constraints resulted in larger calculations that did not improve the description of the long-range interaction, and degraded the description of the short-range interaction. We do not require the O atoms to be spherical at long range here, but use a supermolecule to define the asymptotic energy for each state.

$C_5$  is positive for the  $^1\Pi_g$ ,  $^3\Pi_u$  and  $^5\Pi_g$  states. Hence at long range this is the dominant term and these states are noticeably more bound than the other states of  $O_2$ —see Figs. 1 and 2. In fact, for  $r$  values longer than about  $5 a_0$ , the  $^5\Pi_g$  state is the lowest-lying state of  $O_2$ . This, coupled with the high degeneracy of the state, led to the speculation concerning the importance of this state as a precursor for the formation of the  $b^1\Sigma_g^+$  state and  $O(^1S)$  states. As discussed by Wright and in detail by Bates, the importance of this state as an intermediate is strongly dependent upon its  $D_e$  value. Using the  $[5s\ 4p\ 3 + 1d\ 2f\ 1g] + (sp)$  basis set employed for the other states of  $O_2$ , we obtain a  $D_e$  of 0.131 eV at the MRCI+Q level. This is significantly less than the 0.22 eV obtained at the first-order CI (FOCI) level. Because of the possible significance of this state in explaining the details of a number of processes, it is important to calibrate the accuracy of our calculations.

The results of our calibration study for the  $^5\Pi_g$  state are given in Table IV. First, we note that the inclusion of  $2s$  correlation substantially deepens the well and decreases  $r_e$ . The difference with the effect on the ground state occurs because the atomic correlation terms involving  $2s$  to  $3d$  excitation with a recoupling of the  $2p$  electrons are still present at  $r_e$ . In fact the  $2p$  recoupling allows some additional bonding, thus  $2s$  correlation increases the bonding energy for the  $^5\Pi_g$  state. Second, while the magnitude of the Davidson correction is similar to that for

the experimentally characterized states, the relative magnitude of the correction is substantial—it more than doubles the well depth. While corrections of this type and of a similar magnitude have been shown to be accurate for other weakly bound systems, it is important to calibrate the correction for this state, as full CI studies have demonstrated that the Davidson correction can overestimate the effect of higher excitations. This was done by performing expanded reference calculations at the eight-electron level using the  $[4s\ 3p\ 2d\ 1f]$  basis set. A second  $p$  shell was added to the CASSCF active space, CASSCF( $2p,2p'$ ), and then an MRCI was performed with a reference list consisting of all CSFs that could be formed by distributing the eight electrons in all ways among the  $3\sigma_g$ ,  $4\sigma_g$ ,  $3\sigma_u$ ,  $1\pi_u$ ,  $2\pi_u$  and  $1\pi_g$  orbitals. That is, the antibonding orbitals of the second  $p$  shell are not included in constructing the reference space. The MRCI based on this expanded reference space is considerably (0.021 eV) deeper than the smaller MRCI, but the MRCI+Q result is only 0.002 eV shallower than the previous MRCI+Q result. In addition, using the smaller active space and the  $[5s\ 4p\ 3 + 1d\ 2f\ 1g] + (sp)$  basis set, the ACPF and MRCI+Q results are again nearly the same—the ACPF  $D_e$  is 0.003 eV smaller. These results suggest that even at the eight-electron level the MRCI+Q results are reliable for the  $^5\Pi_g$  state. Since the importance of higher excitations will increase when  $2s$  correlation is included, it is likely that the +Q correction is actually an underestimate at the twelve-electron level. This is supported by the ACPF results, which yield a  $D_e$  0.021 eV larger than the MRCI+Q result. If the  $2s$  orbitals and electrons are included in the active space, CASSCF( $2s,2p$ ), and this CASSCF used as the reference space, then  $D_e$  increases by 0.011 and 0.015 eV at the MRCI+Q and ACPF levels, respectively. However, based on accurate calculations on  $N_2$ , we believe that the CASSCF( $2s,2p$ ) reference MRCI+Q and ACPF calculations may overestimate the effect of higher excitations somewhat. Nevertheless, we can use these results to obtain an error estimate for the  $n$ -particle treatment by assuming that the CASSCF( $2p$ )/MRCI+Q is a lower bound and the CASSCF( $2s,2p$ )/ACPF is an upper bound. Correcting for BSSE we obtain a  $D_e$  of  $0.139 \pm 0.018$ . Basis set improvements will unquestionably increase the calculated  $D_e$ . For the  $X^3\Sigma_g^-$  state, by comparing our best computed result to experiment we observe that the basis set incompleteness is about twice the BSSE, so it could be argued that rather than

subtracting the BSSE we should add it to our computed  $D_e$ , to account for basis set incompleteness. Since this procedure is far from rigorous we have increased our uncertainty estimate by 0.01 eV to account for the uncertainty in our one-particle extrapolation. This leads to our best estimate of  $0.16 \pm 0.03$  eV for the  $D_e$  of the  $^5\Pi_g$  state. This value is slightly larger than our preliminary estimate, quoted by Bates, of  $0.14 \pm 0.03$  eV. While our estimate is smaller than the FOCI result employed by Wraight, it is large enough that it might be necessary to reconsider the importance of the  $^5\Pi_g$  state as a precursor.

In Table IV we compare our computed spectroscopic constants with the FOCI results of Saxon and Liu. Our calculated  $r_e$  is  $0.2 a_0$  longer and  $\omega_e$  is much smaller than the FOCI results—see Fig. 3. The difference is a consequence of the FOCI procedure, not the one-particle basis set or method of optimizing the molecular orbitals, as we obtain similar FOCI results using our basis sets and CASSCF orbitals. The FOCI approach substantially overestimates the interaction energy in the region of the potential well: the curve is not even qualitatively correct. In fact, the FOCI approach overestimates the interaction of many of the weakly bound states in this region. For  $\text{NO}^+$  we also found states for which the FOCI binding energies were substantial overestimates.

The spectroscopic constants for the other weakly bound systems are summarized in Table V. The calculated spectroscopic constants for the  $^5\Sigma_u^-$  and  $^5\Pi_u$  states are in surprisingly good agreement with the FOCI results. However, this agreement must be fortuitous, because all of the binding in these van der Waals bound states arises from the dispersion interaction and the FOCI does not include the simultaneous single excitations required to describe it. Based on previous work on the high spin states of  $\text{N}_2$  and  $\text{NO}$ , we estimate that our calculated  $D_e$  values are accurate to within 20%, with the true potential being deeper than the calculated result. Because of the positive  $C_5$  term, the  $^3\Pi_u$  and  $^1\Pi_g$  states have slightly larger  $D_e$  and shorter  $r_e$  values than the weakly bound states, where  $C_6$  is the first non-zero term in the multipole expansion.

Borrell *et al.* found perturbations in the  $N=9, 11$ , and  $13$  rotational levels of  $v=11$  for the  $A\ ^3\Sigma_u^+$  state. These rotational levels lie between  $61 \pm 15$  and  $15 \pm 15$   $\text{cm}^{-1}$  below the dissociation limit. They suggested, based on the poten-

tials of Saxon and Liu, that the  $^5\Sigma_u^-$  state was the most likely candidate for the perturbing state. Our ACPF  $D_e$  value of  $47\text{ cm}^{-1}$ , which is expected to be up to 20% too small, is not inconsistent with this assignment. We note that the  $^1\Pi_g$  and  $^3\Pi_u$  states cross the  $A^3\Sigma_u^+$  state in this region as well. However, if they were the perturbing states, they would have been expected to affect levels below  $N=9$ , since they have significantly larger  $D_e$  values than the  $^5\Pi_g$  state. Thus our results agree with the hypothesis of Borrell *et al.* that  $^5\Sigma_u^-$  is the most probable candidate for the perturbing state.

#### IV. Conclusions

We have demonstrated that a CASSCF(2p)/MRCI+Q description in a  $[5s\ 4p\ 3d\ 2f\ 1g]$  ANO basis set supplemented with diffuse functions provides a quantitative description of the six lowest states of  $O_2$ . The calculated potentials are within 0.05 eV (1.5 kcal/mol) of the (accurate) experimental results. In addition, we have investigated the importance of substantially expanding the primitive basis set and demonstrated that such expansions yield insignificant improvement in the spectroscopic constants: the expanded basis set recovers 0.57 eV more atomic correlation but  $D_e$  increases by only 0.01 eV.

Potential energy curves have also been reported for the weakly bound states of  $O_2$ . Based on a series of calibration calculations the  $^5\Pi_g$  state is estimated to have a  $D_e$  of  $0.16\pm 0.03$  eV. This estimate is slightly larger than our preliminary estimate, quoted by Bates, but the upper bound of our  $D_e$  is sufficiently large that the importance of this state as a precursor should be reconsidered. The computed spectroscopic constants for the other weakly bound systems are in reasonably good agreement with previous FOCI estimates.

#### Acknowledgments

PRT was supported by NASA Grant NCC 2-371.

Table I. Calibration studies for the  $X^3\Sigma_g^-$ ,  $b^1\Sigma_g^+$ , and  $a^1\Delta_g$  states of  $O_2^a$ .

Basis	$r_e(\text{\AA})$	$\omega_e(\text{cm}^{-1})$	$D_e(\text{eV})$	$T_e(\text{eV})^b$
$X^3\Sigma_g^-$				
$[9s\ 7p\ 4d\ 2f]^c$	1.212(1.215)	1544(1537)	4.982(5.105)	
$[9s\ 7p\ 4d\ 2f]^c\text{-ACPF}$	1.215	1533	5.109	
$[4s\ 3p\ 2d\ 1f]$	1.215(1.218)	1551(1547)	4.879(4.996)	
$[4s\ 3p\ 2d\ 1f]\text{-ACPF}$	1.219	1545	5.002	
$[5s\ 4p\ 3d\ 2f\ 1g]$	1.210(1.214)	1556(1549)	5.041(5.168)	
$[6s\ 5p\ 4d\ 3f\ 2g\ 1h]$	1.208(1.212)	1559(1552)	5.095(5.225)	
$[5s\ 4p\ 3 + 1d\ 2f\ 1g] + (sp)$	1.210(1.213)	1558(1550)	5.065(5.193)	
$[5s\ 5p\ 3d\ 2f\ 1g]$	1.210(1.213)	1556(1550)	5.051(5.177)	
Expt. <sup>d</sup>	1.208	1580	5.214	
$a^1\Delta_g$				
$[5s\ 4p\ 3d\ 2f\ 1g]$	1.220(1.222)	1499(1493)	4.065(4.153)	0.977(1.015)
$[5s\ 4p\ 3 + 1d\ 2f\ 1g] + (sp)$	1.219(1.221)	1500(1495)	4.101(4.179)	0.964(1.014)
$[5s\ 4p\ 3 + 1d\ 2f\ 1g] + (sp)\text{-1root}^e$	1.219(1.221)	1501(1496)	4.091(4.186)	0.960(1.007)
$[5s\ 4p\ 3 + 1d\ 2f\ 1g] + (sp)\text{-ACPF}$	1.222	1494	4.181	
Expt. <sup>d</sup>	1.2156	1484	4.232	0.982
$b^1\Sigma_g^+$				
$[5s\ 4p\ 3d\ 2f\ 1g]$	1.232(1.233)	1445(1444)	3.389(3.509)	1.653(1.659)
$[5s\ 4p\ 3 + 1d\ 2f\ 1g] + (sp)$	1.231(1.232)	1446(1446)	3.425(3.537)	1.640(1.656)
Expt. <sup>d</sup>	1.22688	1433	3.578	1.636

<sup>a</sup> Values in parentheses include a Davidson correction.

<sup>b</sup>  $T_e$  values calculated as the difference in  $D_e$  values.

<sup>c</sup> This is a segmented basis set while all of the other basis sets are based on ANOs—see text.

<sup>d</sup> Ref. X.

<sup>e</sup> CASSCF optimization is for only the  $^1\Delta_g$  state.



Table II. Summary of O<sub>2</sub> Spectroscopic Constants<sup>a</sup>.

	MRCI			MRCI+Q			Expt.		
	$r_e(\text{\AA})$	$\omega_e(\text{cm}^{-1})$	$D_e(\text{eV})$	$r_e(\text{\AA})$	$\omega_e(\text{cm}^{-1})$	$D_e(\text{eV})^b$	$r_e(\text{\AA})$	$\omega_e(\text{cm}^{-1})$	$D_e(\text{eV})$
$X^3\Sigma_g^-$	1.210	1558	5.065	1.213	1550	5.193	1.208	1580	5.214
$a^1\Delta_g$	1.219	1500	4.101	1.221	1495	4.179	1.216	1484	4.232
$b^1\Sigma_g^+$	1.231	1446	3.425	1.232	1446	3.537	1.227	1433	3.578
$c^1\Sigma_u^-$	1.521	754	0.991	1.521	772	1.104	1.514	797	1.114
$A'^3\Delta_u$	1.517	770	0.774	1.517	788	0.881	1.513	815	0.903
$A^3\Sigma_u^+$	1.524	765	0.968	1.524	782	0.804	1.520	804	0.825

<sup>a</sup>Spectroscopic constants computed using the  $[5s\ 4p\ 3 + 1d\ 2f\ 1g] + (sp)$  basis set.

<sup>b</sup>The BSSE error (per atom) is 0.022 eV at 2.3  $a_o$  and 0.013 eV at 2.9  $a_o$ . The tabulated  $D_e$  does not include this correction.

Table III. Calculated energy values for O<sub>2</sub> (in cm<sup>-1</sup>).

$r$	$c^1\Sigma_u^-$	$A'^3\Delta_u$	$A^3\Sigma_u^+$	$^5\Pi_g$	$^3\Pi_u$	$^1\Pi_g$	$^5\Sigma_u^-$	$^5\Pi_u$
2.10	25784.41	27954.91	29276.27					
2.30	5491.75	7408.75	8493.08					
2.50	-4248.81	-2452.53	-1560.47		21041.97			
2.70	-8143.70	-6374.92	-5638.27					
2.80	-8793.02	-7011.36	-6340.75	15902.33	8111.17			
2.90	-8893.33	-7085.20	-6474.02					
3.00	-8615.03	-6770.91	-6212.59			30511.30		
3.01		-6723.72	-6170.39	7334.67	4240.44			
3.10	-8089.77	-6206.20	-5694.97					
3.30	-6676.75	-4729.16	-4296.81					
3.50	-5187.38	-3250.95	-2883.00	-45.36	2016.92	9530.66		6620.31
3.70	-3881.34	-2066.34	-1754.19	-778.25				
3.80				-943.19				
3.90				-1025.92				
4.00	-2424.63	-985.14	-749.31	-1052.98	1169.42	3444.33	4171.39	2342.29
4.10				-1043.47				
4.30				-964.44				
4.40							1752.90	
4.50	-1092.02	-343.33	-213.53	-853.44	297.38	1048.55		752.11
4.70				-739.23				
4.80							694.87	
5.00	-510.45	-170.19	-94.81	-584.91	-90.20	186.92		195.53
5.50	-252.66	-99.45	-52.70	-388.95	-188.69	-80.91	92.17	19.57
5.75					-190.53	-122.98		-11.48
6.00	-133.66	-61.05	-30.06	-258.31	-179.19	-136.78	-5.68	-25.15
6.25						-135.23	-20.94	-29.62
6.50	-75.86	-38.09	-16.58	-173.11	-142.72	-125.97	-26.51	-29.23
6.75							-27.07	
7.00						-100.09	-24.95	-23.48
7.50	-29.88	-16.16	-5.45	-81.80	-78.28	-75.64	-19.61	-16.96
8.00							-13.99	-11.79
8.50	-15.02	-8.91	-3.00		-43.00		-9.67	
9.00		-7.17	-2.78					-7.25
10.00	-7.30	-5.14	-2.66	-19.03	-19.94	-19.83	-3.49	-3.06
12.00							-2.88	
20.00							0.00	0.00
50.00		0.00	0.00	0.00	0.00	0.00		

Table IV. Calibration study for the  $O_2 \ ^5\Pi_g$  Spectroscopic Constants<sup>a</sup>.

	$r_e(a_o)$	$\omega_e(\text{cm}^{-1})$	$D_e(\text{eV})$
12-electron			
[9s 7p 4d 2f]	4.230(4.031)	224(232)	0.067(0.129)
[9s 7p 4d 2f]-ACPF <sup>b</sup>			0.151
[4s 3p 2d 1f]	(4.135)	(194)	(0.099) <sup>c</sup>
[4s 3p 2d 1f]	4.100	197	0.109
[5s 4p 3d 2f 1g]	4.317(4.036)	139(230)	0.056(0.124)
[6s 5p 4d 3f 2g 1h]	(4.023)	(229)	(0.130)
[5s 4p 3 + 1d 2f 1g] + (sp)	4.227(4.022)	222(230)	0.068 <sup>d</sup> (0.131 <sup>e</sup> )
[5s 4p 3 + 1d 2f 1g] + (2s2p1d1f)			(0.136) <sup>f</sup>
[5s 4p 3 + 1d 2f 1g] + (2s2p1d1f)-ACPF			(0.158)
[5s 4p 3 + 1d 2f 1g] + (sp)-ACPF	3.971	237	0.152
[5s 4p 3 + 1d 2f 1g] + (sp)-CASSCF(2s,2p)			0.064(0.142)
[5s 4p 3 + 1d 2f 1g] + (sp)-CASSCF(2s,2p)/ACPF			0.167
[5s 5p 3d 2f 1g]			0.054(0.127)
Saxon and Liu	3.80	350	0.22
8-electron			
[4s 3p 2d 1f]	4.481(4.242)	105(154)	0.048(0.068)
[4s 3p 2d 1f]-CASSCF(2p, 2p')	4.252(4.268)	138(134)	0.079(0.066)
[5s 4p 3 + 1d 2f 1g] + (sp)-MRCI	4.341(4.095)	136(185)	0.061(0.096)
[5s 4p 3 + 1d 2f 1g] + (sp)-ACPF	4.109	185	0.093
[5s 5p 3d 2f 1g]	4.368(4.144)	136(185)	0.056(0.084)

<sup>a</sup>Except where noted these are the MRCI results with the MRCI+Q results given in parentheses using the CASSCF(2p) as a reference.

<sup>b</sup> $D_e$  is calculated using  $r=4.0 \ a_o$ .

<sup>c</sup> Corrected for BSSE, the MRCI+Q  $D_e$  is 0.079 eV.

<sup>d</sup> The MRCI binding energy at  $r=4.0\ a_o$  is 0.054 eV.  
<sup>e</sup> Corrected for BSSE, the MRCI+Q  $D_e$  is 0.121 eV.  
<sup>f</sup> Corrected for BSSE, the MRCI+Q  $D_e$  is 0.122 eV.

Table V. Spectroscopic constants for the weakly bound states of O<sub>2</sub>.

Calculation <sup>a</sup>	$r_e$ ( $a_0$ )	$\omega_e$ (cm <sup>-1</sup> )	$D_e$ (cm <sup>-1</sup> )
<sup>5</sup> Π <sub>u</sub>			
[5s 4p 3 + 1d 2f 1g] + (sp)	6.71(6.63)		36.8(37.3)
[5s 4p 3 + 1d 2f 1g] + (sp)-ACPF	6.66		36.7
Saxon-Liu <sup>b</sup>	7.2		34.0
<sup>5</sup> Σ <sub>u</sub> <sup>-</sup>			
[5s 4p 3 + 1d 2f 1g] + (sp)	6.49(6.24)		31.1(42.8)
[5s 4p 3 + 1d 2f 1g] + (sp)-ACPF	6.15		46.8
Saxon-Liu	6.5		39.5
<sup>3</sup> Π <sub>u</sub>			
[5s 4p 3 + 1d 2f 1g] + (sp)	5.83(5.65)	60(59)	147.0(191.6)
Saxon-Liu	5.5		165.2
<sup>1</sup> Π <sub>g</sub>			
[5s 4p 3 + 1d 2f 1g] + (sp)	6.17(6.09)	57(58)	111.5(137.8)
Saxon-Liu	6.2		117.9

<sup>a</sup>The numbers in parenthesis include a Davidson correction.

<sup>b</sup> Ref. xx

The Structures, Binding Energies and  
Vibrational Frequencies of  $\text{Ca}_3$  and  $\text{Ca}_4$  —  
An Application of the CCSD(T) Method

Timothy J. Lee and Alistair P. Rendell <sup>†</sup>

NASA Ames Research Center, Moffett Field, California 94035

Peter R. Taylor<sup>‡</sup>

ELORET Institute, Palo Alto, California 94303

**Abstract**

The  $\text{Ca}_3$  and  $\text{Ca}_4$  metallic clusters have been investigated using state-of-the art *ab initio* quantum mechanical methods. Large atomic natural orbital basis sets have been used in conjunction with the singles and doubles coupled-cluster (CCSD) method, a coupled-cluster method that includes a perturbational estimate of connected triple excitations, denoted CCSD(T), and the multireference configuration interaction (MRCI) method. The equilibrium geometries, binding energies and harmonic vibrational frequencies have been determined with each of the methods so that the accuracy of the coupled-cluster methods may be assessed. Since the CCSD(T) method reproduces the MRCI results very well, cubic and quartic force fields of  $\text{Ca}_3$  and  $\text{Ca}_4$  have been determined using this approach and used to evaluate the fundamental vibrational frequencies. The infrared intensities of both the  $e'$  mode of  $\text{Ca}_3$  and the  $t_2$  mode of  $\text{Ca}_4$  are found to be small. The results obtained in this study are compared and contrasted with those from our earlier studies on small Be and Mg clusters.

<sup>†</sup> Present Address: SERC Daresbury Laboratory, Daresbury, Warrington WA4 4AD, UK.

<sup>‡</sup> Mailing Address: NASA Ames Research Center, Moffett Field, California 94035

## Introduction

There has been considerable recent interest in the properties of small clusters (see for example Refs. 1-10), motivated principally by two issues. The first is the question of convergence of cluster properties towards the bulk values. Of course some properties will approach the bulk value more quickly than others as the cluster size is increased. The second issue is interaction between theory and experiment. The study of small clusters has progressed very rapidly since accurate experimental studies may be used to evaluate the predictive reliability of different theoretical methods, and then accurate theoretical studies may be used to evaluate or aid in the design of new experimental techniques.

Our studies of small clusters<sup>11,12</sup> have focused on computing the structures, binding energies, vibrational frequencies and infrared intensities of the trimers and tetramers of the alkaline-earth elements beryllium and magnesium using elaborate treatments of electron correlation. We have also examined<sup>13</sup> the equilibrium structures and binding energies of the pentamers, Be<sub>5</sub> and Mg<sub>5</sub>. In the present study we extend our investigations to include Ca<sub>3</sub> and Ca<sub>4</sub>. There are three previous studies<sup>14,15</sup> of Ca<sub>4</sub> (and none of Ca<sub>3</sub>) that have incorporated electron correlation effects. In one Ca<sub>4</sub> study a total binding energy of 18.3 kcal/mol, relative to four Ca atoms, was obtained at the single-reference single and double excitation configuration interaction (CISD) level of theory, including Davidson's correction<sup>16</sup> for higher excitations. In the other, a binding energy of xx.x kcal/mol was obtained using a multireference CI approach (based on SCF orbitals). Based on our previous studies of the Be and Mg clusters, it is likely that even the higher value is a substantial underestimate of the true binding energy.

Another important component of our earlier studies<sup>11-13,17</sup> is the comparison of geometries and binding energies obtained with various electron correlation methods. The *s* - *p* near-degeneracy effects in the alkaline-earth valence shell are very large, and strongly influence the binding in the small clusters. It is not only essential to describe these non-dynamical effects accurately, however, but also to account properly for dynamical correlation in order to obtain reliable binding energies for these systems. Hence the most desirable treatment might appear to be a full valence complete-active-space SCF (CASSCF) calculation followed by a multireference configuration-interaction (MRCI) calculation. This is indeed an excellent level of treatment, but unfortunately it becomes very expensive to apply in large basis sets and at many geometries.

In our studies of the lighter alkaline-earth clusters, we have made extensive use of the single and double excitation coupled-cluster approach (CCSD) corrected with a perturbational estimate of triple excitations (CCSD(T)).<sup>18</sup> The CCSD(T) method performs very well in comparison with MRCI results for the lighter alkaline-earth clusters, and appears to treat both the non-dynamical and dynamical correlation effects in these systems accurately. We have also established the reliability of the CCSD(T) method by full CI comparisons on Be<sub>3</sub>.<sup>20</sup> compared results obtained at the MRCI level of treatment with those obtained using the single and double excitation coupled-cluster (CCSD) approach and the CCSD(T) method, in which a perturbational estimate of the effects of connected triple excitations has been included.<sup>18</sup> In these studies we established that the CCSD(T) method performs very well in reproducing results obtained from the MRCI approach. Based on many comparisons of full configuration interaction (FCI) and MRCI energies,<sup>19</sup> it has been asserted that the MRCI results should be very close to the  $n$ -particle limit, and we have established<sup>20</sup> that the MRCI and CCSD(T) results for Be<sub>3</sub> are indeed very close to the analogous FCI quantities. For comparison purposes, we have again used the CCSD, CCSD(T) and MRCI methods in examining the potential energy surfaces of Ca<sub>3</sub> and Ca<sub>4</sub> so that it may be determined how well the coupled-cluster methods perform for the series of alkaline-earth metals.

In the next section we describe the computational methods employed in this study and in the following section our results are presented and discussed. A comparison of our new results for the Ca clusters and our previous results for the Be and Mg clusters is also given. The final section contains our conclusions.

## Computational methods

Two atomic natural orbital<sup>21</sup> (ANO) basis sets have been used in this study. The (22s 17p) primitive basis set is that of Partridge<sup>22</sup> and was augmented with a (4d 3f) even tempered polarization set defined by  $\alpha = 2.5^n \alpha_0$  for  $n = 0, \dots, k$ . The  $\alpha_0$  values for the  $d$  and  $f$  functions are 0.0232 and 0.0440, respectively. The smallest basis set consists of 5s, 4p and 1d ANOs and will be denoted [5s 4p 1d]. The larger basis consists of 6s, 5p, 2d and 1f ANOs and will be denoted [6s 5p 2d 1f]. The ANO contraction coefficients were obtained by averaging the natural orbitals from single and double configuration interaction (CISD) calculations on the lowest <sup>1</sup>S and <sup>1</sup>P states of atomic Ca. Only the pure spherical



harmonic components of the  $d$  and  $f$  functions have been used.

As discussed in the Introduction, the CCSD, CCSD(T) and MRCI methods have been used to treat electron correlation. In all cases, only the Ca 4s electrons have been included in the correlation procedure. The coupled-cluster wave functions are based on self-consistent field (SCF) molecular orbitals while the MRCI wave functions are based on CASSCF molecular orbitals. All valence electrons were allowed variable occupancy in all valence orbitals in the CASSCF calculations. References for the MRCI wave functions were selected using a 0.05 threshold — that is, all occupations having a component spin-coupling with a coefficient of 0.05 or larger in the CASSCF wave function were used as references in the MRCI procedure.

In analogy with small Be and Mg clusters, the equilibrium geometries of  $\text{Ca}_3$  and  $\text{Ca}_4$  were constrained to have  $D_{3h}$  and  $T_d$  symmetry, respectively. Harmonic frequency analyses demonstrate explicitly that these geometries are indeed minima on the  $\text{Ca}_3$  and  $\text{Ca}_4$  potential energy surfaces. In addition, a linear structure for  $\text{Ca}_3$  was optimized and found to be significantly higher in energy than the equilateral triangle. Hence it is expected that the equilateral triangle and tetrahedron are the global minima on the  $\text{Ca}_3$  and  $\text{Ca}_4$  potential energy surfaces, respectively.

The quadratic, cubic and quartic force constants of  $\text{Ca}_3$  and  $\text{Ca}_4$  have been determined numerically and are given in symmetry internal coordinates. The symmetry internal coordinate definitions are:

**$\text{Ca}_3$**

$$S_1(a'_1) = \frac{1}{\sqrt{3}}(r_1 + r_2 + r_3) \quad (1)$$

$$S_{2a}(e') = \frac{1}{\sqrt{6}}(2r_1 - r_2 - r_3) \quad (2)$$

$$S_{2b}(e') = \frac{1}{\sqrt{2}}(r_2 - r_3) \quad (3)$$

**$\text{Ca}_4$**

$$S_1(a_1) = \frac{1}{\sqrt{6}}(r_1 + r_2 + r_3 + r_4 + r_5 + r_6) \quad (4)$$

$$S_{2a}(e) = \frac{1}{\sqrt{12}}(2r_1 - r_2 - r_3 + 2r_4 - r_5 - r_6) \quad (5)$$

$$S_{2b}(e) = \frac{1}{\sqrt{4}}(r_2 - r_3 + r_5 - r_6) \quad (6)$$

$$S_{3x}(t_2) = \frac{1}{\sqrt{2}}(r_2 - r_5) \quad (7)$$

$$S_{3y}(t_2) = \frac{1}{\sqrt{2}}(r_3 - r_6) \quad (8)$$

$$S_{3z}(t_2) = \frac{1}{\sqrt{2}}(r_1 - r_4). \quad (9)$$

For  $\text{Ca}_4$ , the numbering of bonds is such that if  $r_1$  connects one pair of atoms,  $r_4$  connects the other pair, and similarly for the pairs  $\{r_2, r_5\}$  and  $\{r_3, r_6\}$ . According to convention,<sup>23</sup> the  $a$  component of the doubly degenerate coordinates is defined such that it is symmetric with respect to a  $\sigma_v$  reflection plane, whereas the  $b$  component is antisymmetric. The  $x$ ,  $y$  and  $z$  components of the triply degenerate coordinate are also defined according to established convention.<sup>24</sup>

The precision of the central difference numerical procedures used to obtain the force constants has been closely monitored: the uncertainty in the harmonic frequencies should be less than  $0.1 \text{ cm}^{-1}$  and in the fundamental frequencies less than  $0.5 \text{ cm}^{-1}$ . The anharmonic analyses have been performed with the SPECTRO program package<sup>25</sup> which uses second-order perturbation theory;  $\text{Ca}_3$  has been treated as a symmetric top<sup>23</sup> and  $\text{Ca}_4$  has been treated as a spherical top.<sup>26</sup> The coupled-cluster calculations were performed with the TITAN set of programs<sup>27</sup> interfaced to the MOLECULE-SWEDEN suite of programs.<sup>28</sup> The MRCI calculations were performed with MOLECULE-SWEDEN.

## Results and Discussion

### A. Equilibrium structures and binding energies

Table 1 contains the equilibrium bond distances, rotational constants and dissociation energies (atomization energies) of  $\text{Ca}_3$  and  $\text{Ca}_4$  computed in this study. For  $\text{Ca}_3$  the CCSD level of theory substantially underestimates the  $D_e$  value (i.e.,  $5.7 \text{ kcal/mol}$  or  $47\%$  compared to MRCI) and therefore yields a bond length  $0.22 a_0$  too long. However, the CCSD(T) level of theory exhibits a significant improvement over the CCSD results:  $D_e$  is only  $0.9 \text{ kcal/mol}$  less than the MRCI result and the equilibrium bond distance differs from the MRCI value by only  $0.01 a_0$ . A similar situation is found with  $\text{Ca}_4$  — the CCSD level of theory substantially underestimates the binding energy and gives an equilibrium bond distance  $0.11 a_0$  too long. However, as was found for the Be and Mg clusters,<sup>11,12</sup> the CCSD level of theory performs better for  $\text{Ca}_4$  than it does for  $\text{Ca}_3$ . The CCSD(T)

results for  $\text{Ca}_4$  (using the smaller ANO basis set) are in very good agreement with the respective MRCI quantities. The CCSD(T)  $D_e$  is only 0.2 kcal/mol less than the MRCI value and the CCSD(T)  $r_e$  is actually  $0.02 a_0$  shorter than the MRCI  $r_e$ . As with our earlier studies<sup>11,12</sup> of small Be and Mg clusters, it thus appears that the CCSD(T) level of theory provides a very good description of electron correlation effects in small Ca clusters.

It is interesting to note that comparison of the equilibrium bond distances obtained with the CCSD, CCSD(T) and MRCI methods suggests that the bonding in small Ca clusters is intermediate between the bonding in small Be and small Mg clusters, as would be expected based on the bulk binding energies.<sup>29</sup> For  $\text{Be}_3$ , where  $sp$  hybridization is known to play an important role in the binding, the CCSD level of theory yields a reasonable equilibrium bond distance when compared to MRCI or CCSD(T). However, for  $\text{Mg}_3$ , where the binding is more dominated by dispersion, the CCSD level of theory gives a bond distance that is significantly too long ( $0.55 a_0$ ). The discrepancy in the CCSD bond length for  $\text{Ca}_3$  is between that found for  $\text{Be}_3$  and  $\text{Mg}_3$ , but is much closer to the value obtained for  $\text{Be}_3$  than that found for  $\text{Mg}_3$ . It therefore seems that  $sp$  hybridization is an important component of the bonding in  $\text{Ca}_3$ , though not as important as it is in the bonding of  $\text{Be}_3$ .

For  $\text{Ca}_4$ , only the CCSD and CCSD(T) levels of theory could be used in conjunction with the larger ANO basis set since the MRCI procedure would have been prohibitively expensive. Using the  $[6s\ 5p\ 2d\ 1f]$  ANO basis set, the CCSD(T) equilibrium bond distance for  $\text{Ca}_4$  is  $0.29 a_0$  shorter than the analogous  $\text{Ca}_3$  value indicating the increased importance of  $sp$  hybridization in the bonding as the cluster size becomes larger. The best  $D_e$  values for  $\text{Ca}_3$  and  $\text{Ca}_4$  obtained in this work are 12.1 kcal/mol and 31.5 kcal/mol, respectively. As expected, our best computed  $D_e$  for  $\text{Ca}_4$  is substantially larger than the previously best computed value.<sup>14</sup> Based on the fact that the separated-atom limit is described better than the molecule, the  $D_e$  values for  $\text{Ca}_3$  and  $\text{Ca}_4$  are probably underestimated somewhat. We say “probably” because it is not certain whether the effects of core-correlation will increase or decrease the  $D_e$  values. However, based on a recent study of  $\text{Ca}_2$  by Dyall and McLean,<sup>30</sup> it is likely that the effects of core-correlation will not affect the  $D_e$  values by more than 1-2 kcal/mol.

## B. Vibrational frequencies of $\text{Ca}_3$

The quadratic force constants and harmonic frequencies of  $\text{Ca}_3$  obtained at the

CCSD, CCSD(T) and MRCI levels of theory are presented in Table 2. The  $[6s\ 5p\ 2d\ 1f]$  ANO basis set was used with all of these methods. In view of the underestimation of the bond strength at the CCSD level, it is not surprising that the CCSD quadratic force constants and harmonic frequencies are noticeably smaller than the analogous MRCI values. Conversely, the CCSD(T) quadratic force constants and harmonic frequencies are in excellent agreement with the MRCI quantities, being only  $1\text{ cm}^{-1}$  and  $2\text{ cm}^{-1}$  smaller for the  $a'_1$  and  $e'$  modes, respectively. The best computed harmonic frequencies of  $\text{Ca}_3$  obtained in this work are  $95\text{ cm}^{-1}$  and  $85\text{ cm}^{-1}$  for the  $a'_1$  and  $e'$  modes, respectively. These values should be reasonably reliable and are probably low rather than high, assuming that the binding energy is still somewhat underestimated. The harmonic frequencies of  $\text{Ca}_3$  are small not only because the bonding in  $\text{Ca}_3$  is relatively weak, but also because of the large mass of the Ca atom and the  $1/\sqrt{m}$  dependence of the harmonic frequency, where  $m$  is the reduced mass of the system.

We have computed cubic and quartic force constants using the CCSD(T) method, since the CCSD(T) and MRCI harmonic frequencies are in excellent agreement and the former approach is significantly cheaper. The complete set of cubic and quartic force constants and the resulting anharmonic constants are presented in Table 3. Table 4 contains the fundamental vibrational frequencies of  $\text{Ca}_3$  determined via second-order perturbation theory. In addition, Table 4 presents the infrared (IR) intensity of the  $e'$  vibration determined using the double harmonic approximation.

The absolute anharmonic contribution to the vibrational frequencies is small, only  $2\text{ cm}^{-1}$  for both vibrations, and the percentage effect is about half that observed previously for the Mg clusters. Combining the MRCI harmonic frequencies with the anharmonic correction obtained with the CCSD(T) method gives  $93\text{ cm}^{-1}$  and  $83\text{ cm}^{-1}$  as our best estimates for the fundamental vibrational frequencies of the  $a'_1$  and  $e'$  modes, respectively. Because the IR intensity of the  $e'$  mode is so small, the best prospect for determining the vibrational frequencies experimentally is likely to be an indirect technique such as negative ion photoelectron spectroscopy.

### C. Vibrational frequencies of $\text{Ca}_4$

The quadratic force constants and harmonic frequencies of  $\text{Ca}_4$ , determined at the CCSD, CCSD(T) and MRCI levels of theory, are presented in Table 5. A noteworthy point

is that the CCSD harmonic frequencies are in better agreement with the MRCI values than was found for  $\text{Ca}_3$ . This is especially true for  $\omega_2$  and  $\omega_3$  where the differences are only  $4\text{ cm}^{-1}$  and  $8\text{ cm}^{-1}$ , respectively. This observation supports our earlier analysis regarding the increased importance of  $sp$  hybridization, and consequently covalent bonding, in  $\text{Ca}_4$  relative to  $\text{Ca}_3$ . The CCSD(T) quadratic force constants and harmonic frequencies are in excellent agreement with the respective MRCI quantities. Indeed,  $\omega_1$  and  $\omega_2$  only differ by  $1\text{ cm}^{-1}$  and  $\omega_3$  differs by less than this. These comparisons suggests that the CCSD(T) level of theory is closely approaching the  $n$ -particle limit for  $\text{Ca}_4$ .

The CCSD and CCSD(T) harmonic frequencies obtained with the larger  $[6s\ 5p\ 2d\ 1f]$  ANO basis set demonstrate the importance of using large one-particle basis sets in order to obtain highly accurate harmonic frequencies. The difference between the CCSD(T) harmonic frequencies in the two basis sets used is larger than the differences due to correlation treatment among the small basis results. As with  $\text{Ca}_3$ , it is expected that the CCSD(T)/ $[6s\ 5p\ 2d\ 1f]$  quadratic force constants and harmonic frequencies should be very reliable.

Table 6 contains the complete cubic and quartic force field of  $\text{Ca}_4$  obtained at the CCSD(T) level of theory with the larger ANO basis set. The resulting anharmonic constants are given in Table 7, while the fundamental vibrational frequencies and IR intensities of  $\text{Ca}_4$  are presented in Table 8. As with  $\text{Ca}_3$ , the absolute anharmonic corrections for the vibrational modes of  $\text{Ca}_4$  are relatively small at only  $3\text{ cm}^{-1}$ ,  $1\text{ cm}^{-1}$  and  $1\text{ cm}^{-1}$  for  $\omega_1$ ,  $\omega_2$  and  $\omega_3$ , respectively. The percentage effect on the fundamental frequencies is also similar to that found for  $\text{Ca}_3$ . The IR intensity of the  $t_2$  vibration is  $2.1\text{ km/mol}$ , which is substantially larger than the IR intensity of the  $e'$  vibration in  $\text{Ca}_3$ , but again the best method to obtain fundamental frequencies from experiment may be an indirect approach.

#### D. Summary of CCSD(T) Results for Small Be, Mg and Ca Clusters

A summary of the equilibrium structures, vibrational frequencies, infrared intensities and binding energies for the alkaline-earth trimers is presented in Table 9 and for the tetramers in Table 10. The beryllium and magnesium cluster results are taken from our previous studies.<sup>11,12</sup> In all cases, the results are those obtained with the largest ANO basis set used in the particular investigation. For the trimers, Table 9 contains the MRCI equilibrium bond distance, harmonic frequencies and dissociation energy. The fundamental

frequencies were obtained by adding the CCSD(T) anharmonicity to the MRCI harmonic frequencies. The IR intensities were determined with the CCSD(T) method. For the tetramers, all of the results were obtained at the CCSD(T) level of theory since it was not possible to use the MRCI method in conjunction with the larger ANO basis sets for the tetramers. Thus the values summarized in Tables 9 and 10 represent the best computed quantities to date for the alkaline-earth trimers and tetramers.

Examination of the binding energies in Table 9 indicates the expected trend based on bulk binding energies — that is the binding energies decrease in the order  $\text{Be}_3 > \text{Ca}_3 > \text{Mg}_3$ . The vibrational frequencies, on the other hand, decrease in the order  $\text{Be}_3 > \text{Mg}_3 > \text{Ca}_3$ , but this is determined in large part by mass effects, since the symmetry internal coordinate quadratic force constants for  $\text{Mg}_3$  are smaller<sup>12</sup> than those for  $\text{Ca}_3$ . The IR intensity of the  $e'$  mode is small for all of the alkaline-earth trimers.

Comparison of the  $D_e$  values of the tetramers shows the same trend as observed for the trimers, although the ratios are somewhat different. The binding energy of  $\text{Be}_4$  is significantly larger than that of  $\text{Be}_3$ , though the  $\text{Be}_4$  equilibrium bond distance is only  $0.28 a_0$  shorter than the  $\text{Be}_3$  value. The ratio  $D_e(\text{M}_4)/D_e(\text{M}_3)$  is largest for  $\text{M} = \text{Mg}$  and it is therefore not surprising that  $\text{Mg}_4$  exhibits the largest reduction in bond length ( $0.50 a_0$ ) relative to the trimer. The reduction in the  $\text{Ca}_4$  bond length (relative to the trimer) is about the same as that observed for Be even though the ratio  $D_e(\text{M}_4)/D_e(\text{M}_3)$  is significantly larger for  $\text{M} = \text{Be}$  than for  $\text{M} = \text{Ca}$ . This last observation is probably due to the fact that the valence orbitals of Ca are larger than those of Be.

The harmonic frequencies of the tetramers exhibit the same trend as observed for the trimers. Again, the  $\text{Mg}_4$  vibrational frequencies are higher than the analogous  $\text{Ca}_4$  values because of the mass effect. The fundamental frequency  $\nu_3$  for  $\text{Be}_4$  has a large *positive* anharmonic correction that is not observed in either  $\text{Mg}_4$  nor  $\text{Ca}_4$ . This  $\text{Be}_4$  phenomenon was explained in some detail previously,<sup>11</sup> and relies on a symmetry argument applicable to tetrahedral  $\text{X}_4$  species. Its apparent inapplicability to  $\text{Mg}_4$  and  $\text{Ca}_4$  is probably due to several factors, including the much weaker bonds present in  $\text{Mg}_4$  and  $\text{Ca}_4$  relative to  $\text{Be}_4$ . The IR intensities of the tetramer  $t_2$  vibrations are much larger than those calculated for the trimers. Nevertheless, the  $\text{Mg}_4$  and  $\text{Ca}_4$  intensities remain very small and it is likely that the best prospect for experimental determination of these frequencies will be an indirect method like negative ion photodetachment. On the other hand, the IR intensity

of the  $t_2$  mode of  $\text{Be}_4$  is certainly large enough to allow direct experimental observation provided that an experiment can be designed which will produce enough  $\text{Be}_4$ .

## Conclusions

The CCSD, CCSD(T) and MRCI electron correlation methods have been used to investigate the equilibrium structures, vibrational frequencies and binding energies of the  $\text{Ca}_3$  and  $\text{Ca}_4$  metallic clusters. In agreement with our earlier studies of the analogous Be and Mg clusters, it is found that the CCSD(T) method reproduces the MRCI  $r_e$ , harmonic frequencies and  $D_e$  values very well. The agreement between these methods is somewhat better for  $\text{Ca}_4$ , but is still very good for  $\text{Ca}_3$ . Complete cubic and quartic force fields of  $\text{Ca}_3$  and  $\text{Ca}_4$  have been determined with the CCSD(T) method in conjunction with a large ANO basis set and have been used to evaluate the anharmonic corrections needed to compute the fundamental frequencies. The anharmonic corrections have been determined via second-order perturbation theory. The absolute value of the anharmonic corrections is relatively small, although as a percentage relative to the fundamental frequencies they are similar to those observed previously for the Mg clusters. In spite of the fact that Ca is larger and more polarizable than Mg, and that Ca clusters are more strongly bound than Mg clusters, the IR intensities of the  $e'$  mode of  $\text{Ca}_3$  and of the  $t_2$  mode of  $\text{Ca}_4$  are small and similar to the analogous Mg quantities. It is unlikely that direct observation of these fundamentals will be possible.

The MRCI and CCSD(T) equilibrium structures, vibrational frequencies and binding energies of the alkali metal (Be, Mg and Ca) trimers and tetramers have been summarized. The binding energies of the trimers and tetramers follow the bulk metal binding energies although the ratios of the small cluster  $D_e$  values do not agree with the bulk metal ratios. The vibrational frequencies follow a different trend as the  $\text{Mg}_n$  ( $n=3,4$ ) frequencies are larger than the respective Ca values, but this is due to the larger mass of the Ca atom, since the symmetry internal coordinate force constants (which are independent of mass) for the Ca trimer and tetramer are larger than the respective Mg quantities.

## Acknowledgements

PRT was supported by NASA grant NCC 2-371 and APR was supported by an NRC Post-Doctoral Research Fellowship.

## References

1. D. H. Levy, *Annu. Rev. Phys. Chem.* **31**, 197 (1980).
2. A. C. Legon and D. J. Millen, *Chem. Rev.* **86**, 635 (1986).
3. M. M. Kappas *Chem. Rev.* **88**, 369 (1988).
4. D. E. Powers, S. G. Hansen, M. E. Geusic, D. L. Michalopoulos, and R. E. Smalley, *J. Chem. Phys.* **78**, 2866 (1983).
5. T. G. Dietz, M. A. Duncan, D. E. Powers, and R. E. Smalley, *J. Chem. Phys.* **74**, 6511 (1981).
6. S. J. Riley, E. K. Parks, C.-R. Mao, L. G. Pobo, and S. Wexler, *J. Phys. Chem.* **86**, 3911 (1982).
7. C. M. Lovejoy and D. J. Nesbitt, *J. Chem. Phys.* **90**, 4671 (1989).
8. G. T. Fraser, A. S. Pine, R. D. Suernam, D. C. Dayton, and R. E. Miller, *J. Chem. Phys.* **90**, 1330 (1989).
9. J. R. Heath and R. J. Saykally, *J. Chem. Phys.* **94**, 3271 (1991).
10. J. R. Heath, R. A. Sheeks, A. L. Cooksy and R. J. Saykally, *Science* **249**, 895 (1990).
11. A. P. Rendell, T. J. Lee, and P. R. Taylor, *J. Chem. Phys.* **92**, 7050 (1990).
12. T. J. Lee, A. P. Rendell, and P. R. Taylor, *J. Chem. Phys.* **93**, 6636 (1990).
13. T. J. Lee, A. P. Rendell, and P. R. Taylor, *J. Chem. Phys.* **92**, 489 (1990).
14. C. W. Bauschlicher, P. S. Bagus, and B. N. Cox, *J. Chem. Phys.* **77**, 4032 (1982).
15. P. S. Bagus, C. J. Nelin, and C. W. Bauschlicher, *Surface Sci.* **156**, 615 (1985).
16. S. R. Langhoff and E. R. Davidson, *Int. J. Quantum Chem.* **8**, 61 (1974).
17. T. J. Lee, A. P. Rendell, and P. R. Taylor, *J. Phys. Chem.* **94**, 5463 (1990).
18. K. Raghavachari, G. W. Trucks, J. A. Pople, and M. Head-Gordon, *Chem. Phys. Lett.* **157**, 479 (1989).
19. C. W. Bauschlicher, S. R. Langhoff, and P. R. Taylor, *Adv. Chem. Phys.* **77**, 103 (1990).
20. J. D. Watts, I. Cernusak, J. Noga, R. J. Bartlett, C. W. Bauschlicher, T. J. Lee, A. P. Rendell, and P. R. Taylor, *J. Chem. Phys.* **93**, 8875 (1990).
21. J. Almlöf and P. R. Taylor, *J. Chem. Phys.* **86**, 4070 (1987).
22. H. Partridge, *J. Chem. Phys.* **90**, 1043 (1989).



23. I. M. Mills in "Molecular Spectroscopy: Modern Research", edited by K. N. Rao and C. W. Mathews (Academic, New York 1972) Vol. I, pp. 115-140.
24. D. L. Gray and A. G. Robiette, Mol. Phys. **37**, 1901 (1979).
25. J. F. Gaw, A. Willetts, W. H. Green and N. C. Handy, SPECTRO program, version 1.0 (1989).
26. D. P. Hodgkinson, R. K. Heenan, A. R. Hoy, A. G. Robiette, Mol. Phys. **48**, 193 (1983).
27. TITAN is a set of electronic structure programs, written by T. J. Lee, A. P. Rendell and J. E. Rice.
28. MOLECULE-SWEDEN is an electronic structure program system written by J. Almlöf, C. W. Bauschlicher, M. R. A. Blomberg, D. P. Chong, A. Heiberg, S. R. Langhoff, P.-Å. Malmqvist, A. P. Rendell, B. O. Roos, P. E. M. Siegbahn, and P. R. Taylor.
29. J. Donohue, *The Structure of the Elements* (Interscience, New York, 1974).
30. K. G. Dyall, A. D. McLean, private communication.

**Table 1**  
Total energies ( $E_h$ ), bond lengths ( $a_0$ ), rotational  
constants (MHz) and binding energies (kcal/mol) for  $\text{Ca}_3$  and  $\text{Ca}_4$ .

		Basis	$E^a$	$r_e$	$A$	$B$	$D_e$	$D_0$
$\text{Ca}_3$	CCSD	$[6s\ 5p\ 2d\ 1f]$	0.370728	8.097	1378	689	6.4	6.1
	CCSD(T)	$[6s\ 5p\ 2d\ 1f]$	0.378316	7.884 <sup>b</sup>	1453	726	11.2	10.8
	MRCI	$[6s\ 5p\ 2d\ 1f]$	0.379234	7.874	1457	728	12.1	11.7
$\text{Ca}_4$	CCSD	$[5s\ 4p\ 1d]$	0.168123	7.935	717		14.3	13.6
	CCSD(T)	$[5s\ 4p\ 1d]$	0.180604	7.806	741		22.2	21.4
	MRCI	$[5s\ 4p\ 1d]$	0.179059	7.824	738		22.4	21.7
	CCSD	$[6s\ 5p\ 2d\ 1f]$	0.180579	7.694	763		20.9	20.1
	CCSD(T)	$[6s\ 5p\ 2d\ 1f]$	0.197496	7.591 <sup>c</sup>	784		31.5	30.6

<sup>a</sup> The energy for  $\text{Ca}_3$  is reported as  $-(E+2030)$  and for  $\text{Ca}_4$  as  $-(E+2707)$ .

<sup>b</sup> Vibrationally averaged bond lengths:  $r_g = 7.917\ a_0$  and  $r_\alpha = 7.915\ a_0$ .

<sup>c</sup> Vibrationally averaged bond lengths:  $r_g = 7.615\ a_0$  and  $r_\alpha = 7.613\ a_0$ .

**Table 2**

Symmetry internal coordinate force constants ( $\text{aJ}/\text{\AA}^2$ )  
and harmonic frequencies ( $\text{cm}^{-1}$ ) for  $\text{Ca}_3$ .

	$F_{11}$	$F_{22}$	$\omega_1(a'_1)$	$\omega_2(e')$
CCSD	0.04415	0.08141	75	72
CCSD(T)	0.06952	0.10835	94	83
MRCI	0.07126	0.11460	95	85

**Table 3**

Non-zero cubic ( $\text{aJ}/\text{\AA}^3$ ) and quartic ( $\text{aJ}/\text{\AA}^4$ ) force constants and the anharmonic constants ( $\text{cm}^{-1}$ ) for  $\text{Ca}_3$ .

$F_{111}$	-0.133
$F_{12a2a} = F_{12b2b}$	-0.152
$F_{2a2a2a} = -F_{2a2b2b}$	-0.105
$F_{1111}$	0.156
$F_{112a2a} = F_{112b2b}$	0.163
$F_{12a2a2a} = -F_{12a2b2b}$	0.116
$F_{2a2a2a2a} = F_{2b2b2b2b} = 3F_{2a2a2b2b}$	0.239

#### Anharmonic Constants

$x_{11}$	-0.60
$x_{21}$	-1.38
$x_{22}$	-0.41
$g_{22}$	0.18

**Table 4**

Comparison of the CCSD(T) harmonic and fundamental frequencies of  $\text{Ca}_3$  ( $\text{cm}^{-1}$ ). Infrared intensities ( $\text{km/mol}$ ) are also included.

Mode	$\omega$	$\nu$	$\omega - \nu$	I
$a'_1$	94	92	2	0
$e'$	83	81	2	0.4

**Table 5**  
Symmetry internal coordinate quadratic force constants (aJ/Å<sup>2</sup>)  
and harmonic frequencies (cm<sup>-1</sup>) for Ca<sub>4</sub>.

	Basis	$F_{11}$	$F_{22}$	$F_{33}$	$\omega_1(a_1)$	$\omega_2(e)$	$\omega_3(t_2)$
CCSD	[5s 4p 1d]	0.05350	0.12546	0.08688	95	73	86
CCSD(T)	[5s 4p 1d]	0.07166	0.14253	0.10439	110	78	94
MRCI	[5s 4p 1d]	0.06960	0.14091	0.10397	109	77	94
CCSD	[6s 5p 2d 1f]	0.07463	0.15725	0.11282	113	82	98
CCSD(T)	[6s 5p 2d 1f]	0.09446	0.17250	0.13062	127	86	105

**Table 6**  
Non-zero cubic (aJ/Å<sup>3</sup>) and quartic (aJ/Å<sup>4</sup>) force  
constants for Ca<sub>4</sub>.

$F_{111}$	-0.110
$F_{12a2a} = F_{12b2b}$	-0.140
$F_{13x3x} = F_{13y3y} = F_{13z3z}$	-0.126
$F_{2a2a2a} = -F_{2a2b2b}$	-0.074
$F_{2a3z3z} = -2F_{2a3x3x} = -2F_{2a3y3y} = \frac{2}{\sqrt{3}}F_{2b3x3x} = \frac{-2}{\sqrt{3}}F_{2b3y3y}$	-0.190
$F_{3x3y3z}$	-0.013
$F_{1111}$	0.077
$F_{112a2a} = F_{112b2b}$	0.091
$F_{113x3x} = F_{113y3y} = F_{113z3z}$	0.076
$F_{12a2a2a} = -F_{12a2b2b}$	0.058
$F_{12a3z3z} = -2F_{12a3x3x} = -2F_{12a3y3y} = \frac{2}{\sqrt{3}}F_{12b3x3x} = \frac{-2}{\sqrt{3}}F_{12b3y3y}$	0.119
$F_{13x3y3z}$	-0.001
$F_{2a2a2a2a} = F_{2b2b2b2b} = 3F_{2a2a2b2b}$	0.162
$F_{2a2a3z3z}$	0.176
$F_{2b2b3z3z}$	0.044
<sup>a</sup> $F_{2a2a3y3y} = F_{2a2a3x3x} = \frac{1}{4}(F_{2a2a3z3z} + 3F_{2b2b3z3z})$	0.077
<sup>a</sup> $F_{2b2b3y3y} = F_{2b2b3x3x} = \frac{1}{4}(3F_{2a2a3z3z} + F_{2b2b3z3z})$	0.143
<sup>a</sup> $F_{2a2b3y3y} = -F_{2a2b3x3x} = \frac{\sqrt{3}}{4}(F_{2a2a3z3z} - F_{2b2b3z3z})$	0.057
$F_{3x3x3x3x} = F_{3y3y3y3y} = F_{3z3z3z3z}$	0.262
$F_{3x3x3y3y} = F_{3x3x3z3z} = F_{3y3y3z3z}$	0.043

<sup>a</sup> Dependent force constants related to  $F_{2a2a3z3z}$  and  $F_{2b2b3z3z}$ .

**Table 7**  
Anharmonic constants ( $\text{cm}^{-1}$ ) for  $\text{Ca}_4$ .

Anharmonic Constants	
$x_{11}$	-0.31
$x_{21}$	-0.52
$x_{22}$	-0.13
$x_{31}$	-0.83
$x_{32}$	-0.35
$x_{33}$	-0.18
$g_{22}$	0.09
$g_{33}$	0.03
$t_{23}$	-0.05
$t_{33}$	-0.03





**Table 8**

Comparison of the CCSD(T) harmonic and fundamental frequencies of  $\text{Ca}_4$  ( $\text{cm}^{-1}$ ). Infrared intensities ( $\text{km/mol}$ ) are also included.

Mode	$\omega$	$\nu$	$\omega - \nu$	I
$a_1$	127	124	3	0
$e$	86	85	1	0
$t_2$	105	104	1	2.1

**Table 9**Summary of results for the alkaline earth trimers.<sup>a</sup>

	$r_e$	$\omega_1(a'_1)$	$\omega_2(e')$	$\nu_1$	$\nu_2$	$D_e$
Be <sub>3</sub>	4.200	490	427(0.5)	469	410	22.5
Mg <sub>3</sub>	6.373	110	115(0.2)	101	109	6.3
Ca <sub>3</sub>	7.874	95	85(0.4)	93	83	12.1

<sup>a</sup> Units are  $a_0$  for  $r_e$ ,  $\text{cm}^{-1}$  for the harmonic and fundamental frequencies, and kcal/mol for  $D_e$ . The value in parentheses is the IR intensity in km/mol. The Be<sub>3</sub> results are from reference 11 and the Mg<sub>3</sub> results are from reference 12. See text for details of correlation methods used.

**Table 10**  
Summary of CCSD(T) results for the alkaline earth tetramers.<sup>a</sup>

	$r_e$	$\omega_1(a_1)$	$\omega_2(e)$	$\omega_3(t_2)$	$\nu_1$	$\nu_2$	$\nu_3$	$D_e$
Be <sub>4</sub>	3.921	663	469	571(29.7)	639	455	682	79.5
Mg <sub>4</sub>	5.877	192	147	171(2.4)	184	143	167	23.9
Ca <sub>4</sub>	7.591	127	86	105(2.1)	124	85	104	31.5

<sup>a</sup> Units are  $a_0$  for  $r_e$ ,  $\text{cm}^{-1}$  for the harmonic and fundamental frequencies, and kcal/mol for  $D_e$ . The value in parentheses is the IR intensity in  $\text{km/mol}$ . The Be<sub>4</sub> results are from reference 11 and the Mg<sub>4</sub> results are from reference 12.

52-42  
N93-11853

# On the evaluation of derivatives of Gaussian integrals

Trygve Helgaker  
Department of Chemistry  
University of Oslo  
P.O.B. 1033, Blindern  
N-0315 Oslo 3  
NORWAY

and

Peter R. Taylor <sup>†</sup>  
ELORET Institute  
Palo Alto CA 94303  
USA

P - 11  
Ø 2736708  
ET 491029

## Abstract

We show that by a suitable change of variables, the derivatives of molecular integrals over Gaussian-type functions required for analytic energy derivatives can be evaluated with significantly less computational effort than current formulations. The reduction in effort increases with the order of differentiation.

## I. Introduction

Analytic energy derivative methods have revolutionized the application of computational quantum chemistry to problems of chemical interest [1]. The location and characterization of stationary points on polyatomic molecular potential energy surfaces can be accomplished so much more efficiently using analytic derivatives than with techniques based on computing energies alone that the development and extension of analytic derivative methods has been one of the most active fields of methodological research in quantum chemistry in recent years. Given the gradient and Hessian of the energy with respect to the nuclear coordinates, a variety of strategies have been developed that are guaranteed to converge to minima on potential surfaces and that can efficiently locate other stationary points, particularly

---

<sup>†</sup> Mailing address: NASA Ames Research Center, Moffett Field, California 94035-1000

transition states. These strategies can also be used to “walk” on surfaces from one minimum to another, thereby defining a reaction coordinate, and among the most elegant and conceptually illuminating studies of this sort are the investigations of Ruedenberg and co-workers on rearrangement reactions of small hydrocarbon species (see Refs. 2–5 and references therein). It is thus a great pleasure to dedicate this contribution to Professor Ruedenberg on the occasion of his 70th birthday.

Of course, in order to perform such walks and optimizations it is imperative to evaluate the energy derivatives efficiently at the computational level of interest (Hartree-Fock or some correlated treatment). As noted above, much work has been performed in this area, and several reviews are available [1,6,7]. We shall concentrate here on a topic that ultimately affects the computational effort necessary to evaluate energy derivatives for any *ab initio* method that relies on a basis set expansion of Gaussian one-electron functions.

Wave functions for polyatomic molecules are invariably expanded in a basis set that is centred on the various nuclei, and so in a calculation of the energy derivative of  $n$ th order with respect to the nuclear coordinates, up to  $n$ th-order derivatives of the one- and two-electron integrals are required. These derivative integrals can involve differentiation of the operators as well as differentiation of the basis functions, but the greatest computational problems arise from the differentiation of the basis functions. Like the evaluation of integrals over Gaussians [8,9], the calculation of integrals over *differentiated* Gaussians has been the subject of many investigations and numerous efficient computational schemes have been devised. In this work we show how the efficiency of derivative integral evaluation can be improved by some simple manipulations of variables. We shall briefly review the McMurchie-Davidson scheme [8] for computing Gaussian integrals and derivative integrals, and then show how a change of differentiation variables simplifies the formulas.

## II. Derivative Integral Formulas

We shall expand the Gaussian charge distributions that appear in the integrals in Hermite functions, as described by McMurchie and Davidson [8] (see also Saunders [9]). Let us represent an unnormalized Cartesian Gaussian function centred at  $\vec{A}$  by

$$G_{ijk}(\vec{r}, a, \vec{A}) = x_A^i y_A^j z_A^k \exp(-a r_A^2), \quad (1)$$

where  $x_A = x - A_x$ , etc. We can consider one Cartesian direction, say  $x$ , represented

as

$$G_i(x, a, A_x) = x_A^i \exp(-ax_A^2). \quad (2)$$

The overlap distribution of two such functions is expanded as

$$\begin{aligned} \Omega_{ij}(x, a, b, A_x, B_x) &\equiv G_i(x, a, A_x) G_j(x, b, B_x) \\ &= \sum_{t=0}^{i+j} E_t^{ij}(a, b, A_x, B_x) \Lambda_t(x, p, P_x), \end{aligned} \quad (3)$$

where the Hermite function  $\Lambda_t(x, p, P_x)$  is defined by

$$\Lambda_t(x, p, P_x) = (\partial/\partial P_x)^t \exp(-px_p^2) \quad (4)$$

with

$$\vec{P} = \frac{a}{p} \vec{A} + \frac{b}{p} \vec{B} \quad (5)$$

and

$$p = a + b. \quad (6)$$

The expansion coefficients  $E_t^{ij}(a, b, A_x, B_x)$  are obtained from

$$E_t^{i+1,j} = \frac{1}{2p} E_{t-1}^{ij} - \frac{b}{p} R_x E_t^{ij} + (t+1) E_{t+1}^{ij}, \quad (7)$$

where

$$R_x = A_x - B_x \quad (8)$$

and

$$E_0^{00} = \exp(-\frac{ab}{p} R_x^2). \quad (9)$$

Henceforth we shall not always list the arguments of the expansion coefficients or Hermite functions, but we wish to emphasize here that the expansion coefficients depend on  $a$ ,  $b$ , and  $R_x$  only, while the Hermite functions are independent of  $R_x$ :

$$\Omega_{ij}(x, a, b, A_x, B_x) = \sum_{t=0}^{i+j} E_t^{ij}(a, b, R_x) \Lambda_t(x, p, P_x). \quad (10)$$

In terms of the Hermite functions and expansion coefficients we can express a two-electron integral

$$\begin{aligned} &\iint x_A^i y_A^k z_A^m \exp(-ar_A^2) x_B^j y_B^l z_B^n \exp(-br_B^2) \\ &\times r_{12}^{-1} x_C^{i'} y_C^{k'} z_C^{m'} \exp(-cr_C^2) x_D^{j'} y_D^{l'} z_D^{n'} \exp(-dr_D^2) dr_1 dr_2 \end{aligned} \quad (11)$$

as

$$\begin{aligned}
& \sum_{t=0}^{i+j} E_t^{ij}(a, b, A_x, B_x) \sum_{t'=0}^{i'+j'} E_{t'}^{i'j'}(c, d, C_x, D_x) \\
& \times \sum_{u=0}^{k+l} E_u^{kl}(a, b, A_y, B_y) \sum_{u'=0}^{k'+l'} E_{u'}^{k'l'}(c, d, C_y, D_y) \\
& \times \sum_{v=0}^{m+n} E_v^{mn}(a, b, A_z, B_z) \sum_{v'=0}^{m'+n'} E_{v'}^{m'n'}(c, d, C_z, D_z) \\
& \times (tuv|r_{12}^{-1}|t'u'v'), \tag{12}
\end{aligned}$$

where

$$\begin{aligned}
& (tuv|r_{12}^{-1}|t'u'v') \\
& = \int \int \Lambda_t(x, p, P_x) \Lambda_{t'}(x, q, Q_x) \Lambda_u(y, p, P_y) \Lambda_{u'}(y, q, Q_y) \\
& \quad \times \Lambda_v(z, p, P_z) \Lambda_{v'}(z, q, Q_z) r_{12}^{-1} dr_1 dr_2. \tag{13}
\end{aligned}$$

and  $q$  and  $\vec{Q}$  are defined analogously to  $p$  and  $\vec{P}$  but for the second charge distribution. Thus in practice we evaluate integrals over the Hermite function basis and combine those with the expansion coefficients to give integrals over primitive Gaussians. Some modifications to the form (12) are desirable from the point of view of efficiency, as discussed by Saunders [9], but for schematic purposes we can use (12). The first step, evaluation of the Hermite function integrals, is fast. The second step, which we can regard as a transformation from the Hermite function basis to the Cartesian Gaussian basis, is relatively time-consuming and is certainly more expensive than calculating the Hermite function integrals. Finally, if required, we combine these integrals with basis set contraction coefficients to give the final integrals. In fact, some of the expansion steps can be taken outside the contraction step, with a consequent improvement in efficiency.

In a derivative integral we are interested in derivatives of  $\Omega_{ij}$ :  $\partial\Omega_{ij}/\partial A_x$  and  $\partial\Omega_{ij}/\partial B_x$  for first derivatives, for example. Conventionally, we would differentiate the orbitals (2) first and then expand the overlap distributions of the differentiated orbitals analogously to  $\Omega_{ij}$  above. For example, for the derivative with respect to  $A_x$  we obtain

$$\frac{\partial\Omega_{ij}}{\partial A_x} = \sum_{t=0}^{i+j+1} F_t^{ij} \Lambda_t. \tag{14}$$



Note that the sum here is over more terms than appear in the undifferentiated charge distribution (3) — higher orders of differentiation would increase this summation range further. The new coefficients  $F_t^{ij}$  are defined in terms of the coefficients  $E_t^{ij}$  above by

$$F_t^{ij} = 2aE_t^{i+1,j} - iE_t^{i-1,j}. \quad (15)$$

Analogous coefficients can be defined for higher orders of differentiation or for differentiation with respect to  $B_x$ . In this approach, then, we compute derivative integrals using the same general scheme (12) as for undifferentiated integrals. Since the expansion of the differentiated charge distributions in Hermite functions is longer than for the undifferentiated distributions, the work required to transform from the Hermite function basis to the Cartesian Gaussian basis is greater. Further, as the order of differentiation increases this extra work becomes larger and larger. Hence this approach is not well-suited to higher derivatives.

Let us instead consider differentiation with respect to the variables  $P_x$  and  $R_x$ , for which

$$\frac{\partial}{\partial A_x} = \frac{a}{p} \frac{\partial}{\partial P_x} + \frac{\partial}{\partial R_x} \quad (16)$$

and

$$\frac{\partial}{\partial B_x} = \frac{b}{p} \frac{\partial}{\partial P_x} - \frac{\partial}{\partial R_x}. \quad (17)$$

We recall that the Hermite functions are independent of  $R_x$ , while the expansion coefficients are independent of  $P_x$ . Hence we can expect the expressions for the differentiated charge distributions to be simpler in terms of these variables, although we must eventually transform the derivatives back to the  $A_x, B_x$  representation. We obtain for the derivatives

$$\frac{\partial \Omega_{ij}}{\partial P_x} = \sum_{t=0}^{i+j} E_t^{ij} \frac{\partial \Lambda_t}{\partial P_x} = \sum_{t=0}^{i+j} E_t^{ij} \Lambda_{t+1} \quad (18)$$

and

$$\frac{\partial \Omega_{ij}}{\partial R_x} = \sum_{t=0}^{i+j} \frac{\partial E_t^{ij}}{\partial R_x} \Lambda_t. \quad (19)$$

Denoting  $\partial E_t^{ij} / \partial R_x$  by  $E_t^{ij;1}$ , we obtain the expansion relation

$$E_t^{i+1,j;1} = \frac{1}{2p} E_{t-1}^{ij;1} - \frac{b}{p} (R_x E_t^{ij;1} + E_t^{ij}) + (t+1) E_{t+1}^{ij;1} \quad (20)$$

by differentiating the relation (7) above.

We can make several important observations about these derivative formulas. First, the combination of expansion coefficients and Hermite functions in (18) above is over exactly the same range as the summation to give undifferentiated integrals: the only difference is that the degree of the Hermite function has increased by one. Hence the code required to evaluate this term is the same as required in the undifferentiated case, and the number of operations is also the same. (It is easy to see that this holds true in any order of differentiation for this term.) As we saw above, this is not the case if we differentiate with respect to the variables  $A_x$  and  $B_x$ , because then a linear combination of different degree Hermite functions and expansion coefficients appears.

Second, calculation of the differentiated expansion coefficients  $E_t^{kl;1}$  requires essentially the same code again as for the undifferentiated case, with the obvious addition of an extra term in the expansion relation, and a starting value

$$E_0^{00;1} = -\frac{2ab}{p} R_x E_0^{00}, \quad (21)$$

obtained by differentiating (9). As we noted, the index range of the coefficients that are required is the same as that for the undifferentiated case, so the actual work required to combine Hermite function integrals and expansion coefficients does not increase. (The precomputation of the expansion coefficients themselves is of course a very rapid step.)

Third, in the usual scheme the index range of the program loops over the variables  $t, u, v$  depends on the direction of differentiation (i.e., differentiation with respect to  $A_x, A_y$ , etc). Thus these loops must be executed with different ranges for each of the three directions for first derivative integrals, for example. With our transformation of variables, the loop index ranges become independent of the direction of differentiation, so the program logic is simplified and the overheads are reduced. We may also note here that this approach in no way diminishes the possibilities for vectorizing the calculation of the integral derivatives. Indeed, the simplifications to the program loop structure are likely to enhance these possibilities.

Fourth, we can obtain an additional simplification as follows. Adding (16) and (17) we obtain

$$\frac{\partial}{\partial B_x} = \frac{\partial}{\partial P_x} - \frac{\partial}{\partial A_x}. \quad (22)$$

Now, (in addition to saving one multiplication) this form of the expression for the derivative with respect to  $B_x$  does not depend on the orbital exponents at all. Hence we can delay the transformation to the  $B_x$  derivative until later in the calculation, for example, until after the contraction step, so that the time required for this variable transformation becomes negligible. This is most important for first derivatives, as in any order of differentiation only one term can be treated this way.

In the case of higher derivatives there is a variety of terms to be considered but the scheme remains essentially the same. For example, the  $n$ th-order differentiated expansion coefficients with respect to  $R_x$  are obtained from the recursion formula

$$E_t^{i+1,j;n} = \frac{1}{2p} E_{t-1}^{ij;n} - \frac{b}{p} (R_x E_t^{ij;n} + n E_t^{ij;n-1}) + (t+1) E_{t+1}^{ij;n} \quad (23)$$

with starting values

$$E_0^{00;n+1} = -\frac{2ab}{p} (R_x E_0^{00;n} + n E_0^{00;n-1}) \quad (24)$$

and the identification

$$E_t^{ij;0} = E_t^{ij} \quad (25)$$

Higher derivatives of the Hermite functions with respect to  $P_x$  (19) are trivially obtained. We note further that if the two charge distributions that appear in an integral are differentiated separately, the total savings is the product of the individual reductions in work, since the two differentiations are independent. For multiple differentiation of the same charge distribution, we recall that by using our transformation of differentiation variables the summation range in the Hermite function to Cartesian Gaussian transformation is independent of the order of differentiation. Hence the savings increase as the order of differentiation increases, since in the conventional scheme the work required to accomplish this transformation increases substantially with the order of differentiation. In order to obtain an estimate of what savings are possible, we must also include an estimate of the effort required to transform back to the  $A_x, B_x$  representation. We shall now present operation counts showing that it is always preferable to use our transformation of differentiation variables.

In order to simplify the counting we consider only floating-point operations (multiplication and addition), which are weighted equally. In addition, in our count we have not taken advantage of the possibility of deferring transformation of some

derivatives until after contraction: in effect, we are counting operations only for primitive Gaussians and ignoring any additional savings that might accrue from moving manipulations outside the contraction step. If anything, neglecting this possibility favours the conventional approach to derivative integrals.

We have listed operation counts for differentiation of  $SS$ ,  $PP$ , and  $DD$  distributions in Table 1. We have not included the calculation of the Hermite function integrals, which is fast and contributes the same work to both cases, the conventional approach and our new scheme. Further, the transformation of the second charge distribution in the integral has also been excluded. We see that for the  $SS$  case the total operation count is not much affected by whether or not the transformation of variables is performed. However, for higher angular momentum functions there is a decided advantage to using the transformation of variables, and this advantage is clearly growing with the order of differentiation. As a further illustration of this, we note that for third derivatives of a  $PP$  distribution, for example, the conventional method would require 14 448 operations, while using the transformation of variables the work would be reduced to 8 340 operations: a savings of 42%.

Finally, some other aspects of this scheme deserve comment. We note that

$$\frac{\partial}{\partial R_x} = \frac{b}{p} \frac{\partial}{\partial A_x} - \frac{a}{p} \frac{\partial}{\partial B_x}. \quad (26)$$

Therefore, the operation  $\frac{\partial}{\partial R_x}$  is *not* the same as the differentiation  $\frac{\partial}{\partial A_x} - \frac{\partial}{\partial B_x}$ . But if  $A$  and  $B$  coincide then the differentiation with respect to  $R_x$  does not contribute to the energy derivative: only the differentiation with respect to  $P_x$  contributes. This simplification is already used in the ABACUS program [10]. We also note that the use of translational invariance to reduce the computational labour is not affected by our transformation of variables: for first derivatives, for example, we have

$$\frac{dI}{dP_x} + \frac{dI}{dQ_x} = 0, \quad (27)$$

where  $I$  represents the two-electron integral in (11), from the use of translational invariance.

## Conclusions

We have shown that by employing a transformation of differentiation variables, the work required to evaluate derivative integrals can be substantially reduced. The

advantages of our new approach increase both with the order of differentiation and with the angular momentum of the Gaussian functions involved. Savings will be obtained in the calculation of energy derivatives for any wave function that is expanded in a Gaussian basis. In particular, the economies obtained by applying these methods to the calculation of third or higher derivative integrals will be substantial.

#### Acknowledgements

Helpful discussions with W. Klopper are gratefully acknowledged. PRT was supported by NASA grant NCC 2-371.

## REFERENCES

1. P. Pulay, Adv. Chem. Phys. **69**, 241 (1987).
2. P. Valtazanos, S. T. Elbert, S. Xantheas, and K. Ruedenberg, Theor. Chim. Acta **78**, 287 (1991).
3. S. Xantheas, P. Valtazanos, and K. Ruedenberg, Theor. Chim. Acta **78**, 327 (1991).
4. S. Xantheas, S. T. Elbert, and K. Ruedenberg, Theor. Chim. Acta **78**, 365 (1991).
5. P. Valtazanos and K. Ruedenberg, Theor. Chim. Acta **78**, 397 (1991).
6. T. Helgaker and P. Jørgensen, Adv. Quantum Chem. **19**, 183 (1988).
7. J. F. Gaw and N. C. Handy, Roy. Soc. Chem. Ann. Rep. C, 1984, 291.
8. L. E. McMurchie and E. R. Davidson, J. Comput. Phys. **26**, 218 (1978).
9. V. R. Saunders, in *Methods of Computational Molecular Physics*, eds. G. H. F. Diercksen and S. Wilson (Reidel, Dordrecht, 1983).
10. T. U. Helgaker, J. Almlöf, H. J. Aa. Jensen, and P. Jørgensen, J. Chem. Phys. **84**, 6266 (1986).

Table 1. Operation counts for differentiation.

	<i>SS</i>	<i>PP</i>	<i>DD</i>
First Derivatives			
Hermite/Cartesian Transformation	12	396	4 032
$P_x, R_x$ to $A_x, B_x$ Transformation	9	81	324
Total	21	477	4 356
Conventional	24	672	6 144
Second Derivatives			
Hermite/Cartesian Transformation	42	1 386	14 112
$P_x, R_x$ to $A_x, B_x$ Transformation	93	837	3 328
Total	135	2 223	17 460
Conventional	150	3 678	30 912

<sup>504</sup>  
N93-11854  
<sub>558</sub>

Connected Triple Excitations in Coupled-Cluster  
Calculations of Hyperpolarizabilities: Neon

Julia E. Rice  
IBM Research Division, Almaden Research Center  
650 Harry Rd., San Jose, CA 95120-6099

Gustavo E. Scuseria  
Department of Chemistry  
Rice University, Houston, TX 77251-1892

Timothy J. Lee  
NASA Ames Research Center  
Moffett Field, CA 94035

Peter R. Taylor †  
ELORET Institute  
Palo Alto CA 94303

and

Jan Almlöf  
Department of Chemistry and Supercomputer Institute  
University of Minnesota, Minneapolis, MN 55455

† Mailing address: NASA Ames Research Center, Moffett Field, California 94035-1000



## Abstract

We have calculated the second hyperpolarizability  $\gamma$  of neon using the CCSD(T) method. The accuracy of the CCSD(T) approach has been established by explicit comparison with the single, double and triple excitation coupled-cluster (CCSDT) method using extended basis sets that are known to be adequate for the description of  $\gamma$ . Our best estimate for  $\gamma_0$  of  $110\pm 3$  a.u. is in good agreement with other recent theoretical values and with Shelton's recent experimental estimate of  $108\pm 2$  a.u. Comparison of the MP2 and CCSD(T) hyperpolarizability values indicates that MP2 gives a very good description of the electron correlation contribution to  $\gamma_0$ . We have combined MP2 frequency-dependent corrections with the CCSD(T)  $\gamma_0$  to yield values of  $\gamma(-2\omega; \omega, \omega, 0)$  and  $\gamma^K(-\omega; \omega, 0, 0)$ .

## 1. Introduction

Theoretical determination of hyperpolarizabilities has been a topic of much interest recently, since knowledge of atomic and molecular hyperpolarizabilities is central to the understanding of the non-linear response of matter to light. In particular, organic materials with large hyperpolarizabilities are candidates for applications such as optical switching and second harmonic generation, and there is great potential for interaction between theory and experiment in the study of these systems.

From a theoretical point of view, it is important to understand the requirements for determining accurate hyperpolarizabilities for small systems, because it is possible to use large one-particle basis sets and sophisticated electron correlation treatments for these species, and thereby to evaluate the effects of approximations that will be necessary for the study of the hyperpolarizabilities of larger systems. Hence for small systems it is desirable to estimate the accuracy of the calculated hyperpolarizability. This may be accomplished in two ways. First, the quality of the one and  $n$ -particle approximations used in the calculation can be systematically improved and the convergence of the result can be monitored. This is perhaps the preferred approach from a theoretical standpoint. Alternatively, the theoretical value can be compared directly with experiment, although the possibility of error cancellation between the one and  $n$ -particle approximations must always be borne in mind.

Study of the hyperpolarizabilities of the rare gas atoms has a number of advantages. In particular, for neon sophisticated levels of theory and large one-particle basis sets can be employed. Experimental gas-phase electric-field-induced second harmonic generation data for the rare gases is available over a range of frequencies<sup>1</sup>, which makes extrapolation to the static limit possible for the purposes of comparison with a theoretical static value. In addition, vibrational effects (which have been shown to be non-negligible for some molecular values, see, for example, Refs. 2 and 3) vanish for atoms.

It must be noted, however, that it is a non-trivial task to demonstrate convergence of calculated values for hyperpolarizabilities. Previous work has shown that there can be a much larger electron correlation contribution to hyperpolarizabilities than for linear polarizabilities, and that the contribution of higher excitations is not insignificant (see, for example, Refs. 4–6). For example, in the case of  $\gamma$  of neon, where the effect of electron correlation is about 40 a.u., or 40% of  $\gamma$ , the perturbational estimate of triple excitations contributes 8 a.u. or 20% of the total electron correlation contribution.<sup>4</sup> Since the contribution of higher excitations is so large, the applicability of approximate methods for estimating the effects of higher excitations in hyperpolarizability calculations might be questioned. For example, the single and double excitation coupled-cluster method including an estimate of triple excitations through the fourth and partially the fifth order of perturbation theory, (CCSD(T))<sup>7</sup> has had great success in describing the structure and frequencies of a number of ‘difficult’ chemical systems — that is, systems whose wave functions are not dominated by a single reference.<sup>8,9</sup> This success notwithstanding, it is essential to investigate the utility of this approach specifically for determining accurate hyperpolarizabilities.

The reliability of a correlation treatment is best evaluated by comparison with a full configuration-interaction (CI) calculation in the same one-particle basis set. However, since even at the self-consistent field (SCF) level of theory diffuse  $f$  type functions contribute 10 a.u. to the hyperpolarizability of  $\text{Ne}^4$ , a full CI calibration in a realistic basis set is not feasible. Here, in order to establish the accuracy of the CCSD(T) method for  $\gamma$  of neon, we compare instead to results obtained with the full single, double and triple excitation coupled-cluster method (CCSDT),<sup>10,11</sup> in a basis set which is known to be adequate for the description of hyperpolarizabilities. We can thus assess the accuracy of the computed CCSD(T) value, as well as compare it with experimental and other theoretical values. We note that a previous study has demonstrated that for correlation energies, CCSD(T) is an

excellent approximation to CCSDT.<sup>12</sup>

## 2. Computational Methods

The one-particle basis sets used in this work are similar to those employed previously.<sup>4</sup> They were derived from van Duijneveldt's (13s8p) primitive set<sup>13</sup> augmented with a (6d4f) polarization set, with exponents chosen as an even-tempered sequence  $\alpha = 2.5^n \alpha_0$ ;  $n = 0, \dots, k$  with  $\alpha_0 = 0.20, 0.61$  for the  $d$  and  $f$  functions, respectively. This was contracted to [4s 3p 2d 1f] using atomic natural orbitals.<sup>14</sup> The two outermost sets of  $spd$  functions and the outermost  $f$  function were uncontracted to give basis C, denoted [4+1+1s 3+1+1p 2+1+1d 1+1f]. We use the notation C in order to be consistent with our previous study.<sup>4</sup> Additional diffuse functions were then added by extrapolating from the outermost function in an even-tempered sequence,  $\alpha = 2.5^{-n} \alpha_0$ . For example, the addition of one set of diffuse functions is denoted + (1s1p1d1f). In some calculations the basis was further augmented with two diffuse  $g$  functions with exponents of 0.29 and 0.11. Basis set C was completely uncontracted, and two tight  $d$  functions were included ( $\alpha_d = 123.53, 49.41$ ) for calculations in which core correlation was included. Only the true spherical harmonic components of the basis functions were used throughout.

Energies were calculated using self-consistent field (SCF), single and double excitation coupled-cluster (CCSD) and second-order Møller-Plesset perturbation theory (MP2). The effect of triple excitations was investigated using (a) the CCSD(T) method, which includes an estimate of the triples through fourth and partially fifth order of perturbation theory, based on the CCSD amplitudes in the perturbation energy expressions; (b) the CCSDT method, which explicitly includes all single, double and triple excitations; and (c) the CCSD + T(CCSD) method<sup>15</sup> which includes only the fourth-order perturbation theory contribution based on CCSD amplitudes.

The dipole polarizabilities are defined<sup>16</sup> by the energy response to an applied electric

field of strength  $F$ :

$$E(F) = E_0 - \frac{1}{2}\alpha F^2 - \frac{1}{4!}\gamma F^4 - \frac{1}{6!}\epsilon F^6$$

Electric fields of 0, 0.002, 0.004, 0.008, 0.012, 0.016 and 0.020 a.u. were applied and the energy responses were fitted to the sixth-order polynomial in the field strength. The SCF value of  $\gamma$  obtained from the fit agrees with the SCF value obtained from finite displacements of analytic  $\beta$  values to within 0.1 a.u. Tests of the fit for the correlated values indicate the error in  $\gamma$  due to the fit is less than 0.2 a.u.

The SCF, MP2 and most of the coupled-cluster calculations were performed using the MOLECULE-SWEDEN,<sup>17</sup> CADPAC,<sup>18</sup> and TITAN<sup>19</sup> programs. The CCSDT calculations were performed with a program written by one of us (GES).<sup>11</sup> The SCF energies were converged to  $10^{-13} E_h$  or better and the CCSD and CCSDT energies to  $10^{-12}$ .

### 3. Results and Discussion

The values for the linear polarizability,  $\alpha$  and the hyperpolarizability,  $\gamma$  determined in this work are summarized in Table 1. We note first that the SCF, MP2, CCSD and CCSD(T) results for both  $\alpha$  and  $\gamma$  are essentially identical in basis sets C+(3s3p2d3f) and C+(2s2p1d2f). This establishes that these values are converged with respect to further addition of diffuse *s*, *p*, *d*, and *f* functions in the one-particle basis set. It also verifies that basis C+(2s2p1d2f) is a good choice for comparison of the CCSDT and CCSD(T) results. The CCSDT  $\gamma$  value of 110.9 a.u. in this basis is in very good agreement with that from the CCSD(T) method (111.2 a.u.). This establishes that the (T) correction is a reliable estimate of the contribution from connected triple excitations to the hyperpolarizability of Ne, even though the contribution is large. Comparison of the CCSD(T) and CCSD + T(CCSD) results with the C+(3s3p2d3f) basis shows that the fourth-order correction alone is a substantial overestimate.

The effects of diffuse higher-order angular momentum functions and of core correlation have also been investigated at the CCSD(T) level of theory, in order to improve upon

our previous best computed value of 111 a.u.<sup>4</sup> and to assess further our error estimate of  $\pm 4$  a.u. Uncontraction of the one-particle basis set reduces  $\gamma$  from 111.0 a.u. to 110.3 a.u., and core correlation gives a further reduction of 0.5 a.u. Conversely, diffuse  $g$  functions increase  $\gamma$  by 0.2 a.u. These changes are very similar to the values of  $-0.7$ ,  $-0.5$ , and  $0.2$  a.u., respectively, obtained at the CCSD level of theory, whereas the MP2 values indicate that second-order perturbation theory may underestimate the effects of uncontraction ( $-0.4$  a.u.) and core correlation ( $-0.3$  a.u.). This is consistent with the results for argon,<sup>20</sup> where the CCSD estimate of the reduction in  $\gamma$  due to core correlation is larger than the MP2 value. The CCSD(T) results thus support our earlier conclusions<sup>4</sup> that the combination of further augmentation of the one-particle basis set and further improvement in the treatment of core correlation is likely to have little effect on  $\gamma$ .

The importance of higher than triple excitations also requires discussion. Single and double excitations increase  $\gamma$  by 34 a.u. and triple excitations by a further 9 a.u. However, the coupled-cluster expansion should be rapidly convergent, since all the corresponding disconnected terms are included to infinite order at each level of CC theory. The next most important contribution comes from connected quadruple excitations: these can be expected to contribute substantially less than connected triple excitations. It is highly unlikely that these terms contribute as much as 3 a.u. We have previously established<sup>4</sup> that the CCSD(T) energy, at least, agrees almost perfectly with full CI benchmark results for Ne. We thus arrive at a best estimate of 110 a.u., with an uncertainty of 3 a.u. The latter is almost entirely due to uncertainty in the estimated contribution of connected quadruple (and higher) excitations. We can compare our result with Shelton's most recent estimate of  $108 \pm 2$  a.u.<sup>21</sup> based on extrapolation of electric-field-induced second harmonic generation values. This differs from his earlier static value of  $119 \pm 2$  due to his discovery of a systematic error in some of the measurements.<sup>21</sup> Our value is also in good agreement with other recent theoretical values. These include Maroulis and Thakkar's estimate of

114±9 a.u. based on the double-excitation coupled-cluster method augmented with a perturbational estimate of single and triple excitations, denoted CCD+ST(CCD),<sup>22</sup> as well as Chong and Langhoff's CCSD(T) value of 111.0 a.u.<sup>23</sup>, and 108±5 a.u. from the restricted active space self-consistent field calculations of Jensen and co-workers.<sup>24</sup>

It is clearly much easier to demonstrate convergence for  $\alpha$  than for  $\gamma$ . The electron correlation contribution is smaller (around 11%) for  $\alpha$  and the CCSD(T) and CCSDT values agree to 3 decimal places. The diffuse function requirement is also less stringent than for  $\gamma$ . The largest remaining corrections are for core correlation and uncontraction of the one-particle basis set which decrease  $\alpha$  by 0.013 a.u., or 0.5%. Our best computed value for  $\alpha$  is 2.677 a.u. to which we conservatively assign an uncertainty of 0.015 a.u. This is in excellent agreement with the value of 2.669 a.u. derived from dipole oscillator strength distributions by Kumar and Meath.<sup>25</sup>

Finally, the rather good agreement between the MP2 and CC polarizability and hyperpolarizability suggests that the former method may be useful even where, as is the case for neon, the correlation contributions are large. Because it is much simpler to evaluate dynamic polarizabilities with MP2 than with CC methods, this suggests that an efficient route to reliable frequency-dependent results may be to correct CC static values with MP2 differences between static and dynamic values. It is certainly the case that the MP2 values in themselves would be much more reliable than values obtained using SCF methods to describe the frequency dependence. We may also note that the experimental frequencies are far from resonance, so an error in the frequency-dependent hyperpolarizability arising from the error in the prediction of the poles at the MP2 level of theory is not a matter for concern.

In this work we have combined the MP2 frequency-dependent corrections<sup>26</sup> for  $\gamma(-2\omega; \omega, \omega, 0)$  of neon with our best estimate for the static value and arrive at 112±3 a.u. ( $\lambda=1319$  nm), 113±3 a.u. ( $\lambda=1064$  nm), 124±4 a.u. ( $\lambda=514.5$  nm), to

be compared with experimental second harmonic generation values of  $111.1 \pm 0.8$  a.u.<sup>1</sup>,  $109.9 \pm 0.5$  a.u.<sup>1</sup> and  $122.2 \pm 0.5$  a.u.<sup>21</sup>, respectively. The theoretical results show no negative dispersion (note that the uncertainties in the theoretical numbers are not independent and are likely to be strongly correlated with one another), and are also in good agreement with the revised experimental values. We may also combine the MP2 frequency-dependent correction<sup>26</sup> for  $\gamma^K(-\omega; \omega, 0, 0)$  of neon with our best estimate of the static value and obtain  $113 \pm 3$  a.u. for  $\lambda = 632.8$  nm. This value is somewhat higher than the Kerr effect measurement of  $101 \pm 8$  a.u.<sup>27</sup>

#### 4. Conclusions

We have demonstrated by comparison with full CCSDT results that the CCSD(T) method provides an accurate description of the hyperpolarizability of neon. Since the CCSD(T) method has the advantage of being rather inexpensive, it allows extensive investigation of the one-particle basis set requirements and the core correlation treatment for  $\alpha$  and  $\gamma$  of neon. Our best computed CCSD(T) value for  $\gamma$  of neon, including the effects of multiple sets of diffuse  $s$ ,  $p$ ,  $d$  and  $f$  functions and of core correlation, is 109.8 a.u. After incorporating corrections for diffuse  $g$  functions and a more complete treatment of triple excitations our best estimate is 110 a.u. with an error estimate of 3 a.u. This result is in agreement with all of the most recent theoretical values<sup>22–24</sup> and in line with the static value extrapolated from experimental frequency-dependent measurements.<sup>1,21</sup> Together with our assignment of uncertainty, this fulfils our criteria for establishing the accuracy of the computed value.



## References

1. D.P. Shelton, Phys. Rev. A **42**, 2578 (1990).
2. D.M. Bishop, Rev. Mod. Phys. **62**, 343 (1990).
3. D.M. Bishop and B. Kirtman, J. Chem. Phys. **95**, 2646 (1991).
4. P.R. Taylor, T.J. Lee, J.E. Rice and J. Almlöf, Chem. Phys. Lett. **163**, 359 (1989);  
Chem. Phys. Lett. **xxx**, **xxx** (1991).
5. R.J. Bartlett and G.D. Purvis, Phys. Rev. **A20**, 1313 (1979).
6. G. Maroulis and A.J. Thakkar, J. Chem. Phys. **93**, 652 (1990).
7. K. Raghavachari, G.W. Trucks, J.A. Pople and M. Head-Gordon, Chem. Phys. Lett. **157**, 479 (1989).
8. T.J. Lee and G.E. Scuseria, J. Chem. Phys. **93**, 489 (1990).
9. T.J. Lee, A.P. Rendell and P.R. Taylor, J. Chem. Phys. **92**, 489 (1990).
10. J. Noga and R. J. Bartlett, J. Chem. Phys. **85**, 2779 (1986).
11. G. E. Scuseria and H. F. Schaefer, Chem. Phys. Lett. **152**, 382 (1988).
12. G. E. Scuseria and T. J. Lee, J. Chem. Phys. **93**, 5851 (1990).
13. F. B. van Duijneveldt, IBM Publication RJ945 (1971).
14. J. Almlöf and P.R. Taylor, J. Chem. Phys. **86**, 4070 (1987).
15. M. Urban, J. Noga, S.J. Cole and R.J. Bartlett, J. Chem. Phys. **83**, 4041 (1985).
16. A.D. Buckingham, Adv. Chem. Phys., **12**, 107 (1967).
17. MOLECULE-SWEDEN is an electronic structure program system written by J. Almlöf, C. W. Bauschlicher, M. R. A. Blomberg, D. P. Chong, A. Heiberg, S. R. Langhoff, P.-Å. Malmqvist, A. P. Rendell, B. O. Roos, P. E. M. Siegbahn, and P. R. Taylor.
18. R. D. Amos and J. E. Rice, CADPAC:Cambridge Analytic Derivatives Package, Issue 4.0 (Cambridge University, Cambridge, England, 1987).

19. TITAN is a set of electronic structure programs written by T.J. Lee, A.P. Rendell and J.E. Rice.
20. J.E. Rice, P.R. Taylor, T.J. Lee and J. Almlöf, *J. Chem. Phys.* **94**, 4972 (1991).
21. D.P. Shelton, personal communication and work presented at the North American Chemical Congress (ACS), August, 1991.
22. G. Maroulis and A.J. Thakkar, *Chem. Phys. Lett.* **156**, 87 (1989).
23. D.P. Chong and S.R. Langhoff, *J. Chem. Phys.* **93**, 570 (1990).
24. H.J. Aa. Jensen, P. Jørgensen, H. Hettema and J. Olsen, *Chem. Phys. Lett.*, in press.
25. A. Kumar and W.J. Meath, *Can. J. Chem.*, **63**, 1616 (1985).
26. J.E. Rice, *J. Chem. Phys.*, submitted.
27. A. D. Buckingham and D. A. Dunmur, *Trans. Faraday Soc.*, **64**, 1776 (1968).

**Table 1**  
Neon dipole polarizabilities (a.u.)

Basis set	Method	$\alpha$	$\gamma$
$C^a + (2s2p1d2f)$	SCF	2.377	68.66
	MP2	2.713	110.6
	CCSD	2.643	102.2
	CCSD(T)	2.690	110.9
	CCSDT	2.690	111.2
$C^a + (3s3p2d3f)$	SCF	2.377	68.68
	MP2	2.713	110.7
	CCSD	2.643	102.2
	CCSD + T(CCSD)	2.703	115.3
	CCSD(T)	2.690	111.0
$C^a + (3s3p2d3f2g)$	SCF	2.377	68.67
	MP2	2.716	110.9
	CCSD	2.645	102.4
	CCSD(T)	2.692	111.2
$(13s8p8d4f)+(3s3p2d3f)^b$	SCF	2.377	68.67
	MP2	2.708	110.3
	CCSD	2.636	101.5
	CCSD(T)	2.684	110.3
$(13s8p8d4f)+(3s3p2d3f)^c$	MP2	2.703	110.0
	CCSD	2.628	100.8
	CCSD(T)	2.677	109.8

<sup>a</sup> See text for the definition of C.

<sup>b</sup> Uncontracted basis with 8 electrons correlated

<sup>c</sup> Uncontracted basis with 10 electrons correlated

## Concerted hydrogen atom exchange between three HF molecules

Andrew Komornicki  
Polyatomics Research Institute  
1101 San Antonio Rd. Suite 420  
Mountain View, CA 94043

and

David A. Dixon  
Central Research and Development Department  
E.I. du Pont de Nemours and Co.  
Experimental Station 328  
Wilmington DE 19898  
Contribution No. 4558

and

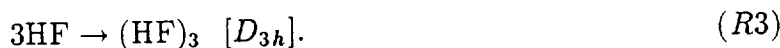
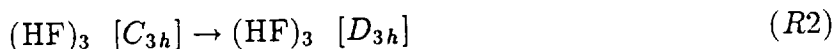
Peter R. Taylor  
ELORET Institute†  
Palo Alto, CA 94303

## ABSTRACT

We have investigated the termolecular reaction involving concerted hydrogen exchange between three HF molecules, with particular emphasis on the effects of correlation at the various stationary points along the reaction. Using an extended basis, we have located the geometries of the stable hydrogen-bonded trimer, which is of  $C_{3h}$  symmetry, and the transition state for hydrogen exchange, which is of  $D_{3h}$  symmetry. The energetics of the exchange reaction were then evaluated at the correlated level, using a large atomic natural orbital basis and correlating all valence electrons. Several correlation treatments were used, namely, configuration interaction with single and double excitations, coupled-pair functional, and coupled-cluster methods. We are thus able to measure the effect of accounting for size-extensivity. Zero-point corrections to the correlated level energetics were determined using analytic second derivative techniques at the SCF level. Our best calculations, which include the effects of connected triple excitations in the coupled-cluster procedure, indicate that the trimer is bound by  $9 \pm 1$  kcal/mol relative to three separated monomers, in excellent agreement with previous estimates. The barrier to concerted hydrogen exchange is 15 kcal/mol above the trimer, or only 4.7 kcal/mol above three separated monomers. Thus the barrier to hydrogen exchange between HF molecules via this termolecular process is very low.

† Mailing address: NASA Ames Research Center, Moffett Field, CA 94035-1000

The HF trimer is known to adopt a  $C_{3h}$  equilibrium structure<sup>4</sup>, while the transition state for concerted hydrogen exchange has been found to display  $D_{3h}$  symmetry. We shall consider the following three reactions:



Clearly, the energies of these three reactions are not independent, but it is convenient to retain all three for purposes of discussion.

There have been a number of recent calculations of the relative energies of the  $C_{3h}$  and  $D_{3h}$  forms of the hydrogen fluoride trimer, that is, the energy of (R2), generally at the self-consistent field (SCF) level. Gaw and coworkers<sup>4</sup> calculated this energy to be 29.5 kcal/mol using a double-zeta plus polarization (DZP) basis. From their data, the actual energy for reaction (R3) to proceed is 14.6 kcal/mol, uncorrected for vibrational effects. Heidrich<sup>5</sup> *et al.* employed a variety of basis sets with geometries obtained by optimization at the 4-31G split-valence level. Their best calculation gave  $\Delta E(D_{3h}-C_{3h}) = 37.1$  kcal/mol (R2) and an activation energy (R3) of 26.5 kcal/mol. An investigation of the relative stability of cyclic and open forms of the trimer by Karpfen<sup>6</sup> and coworkers has shown that the cyclic structure is more stable, while Liu *et al.* have investigated the stabilities of the trimer and tetramer relative to isolated fragments<sup>7</sup>. Most recently, Karpfen<sup>8</sup> has investigated equilibrium structures and concerted hydrogen exchange in  $(\text{HF})_3$  and several other HF clusters, using split-valence plus polarization basis sets and the averaged coupled-pair functional (ACPF) method. These results are compared to ours below.

In the present work we use large segmented Gaussian basis sets to locate the  $(\text{HF})_3$  stationary points at the SCF level, and then refine the energetics by performing extensive correlated calculations at the configuration-interaction and coupled-cluster levels, using large atomic natural orbital basis sets. Our computational methods are described in the next section, followed by a discussion of our results and conclusions.

### Computational methods

The geometry of each stationary point was initially optimized at the SCF level using a triple-zeta plus polarization (TZP) basis of the form  $[5s\ 3p\ 1d]/[3s\ 1p]$  contracted from a  $(10s\ 6p\ 2d/5s\ 1p)$  primitive set<sup>9</sup>. The fluorine  $d$  set is a two-term fit to a Slater function with exponent 2.2 and the hydrogen  $p$  set has a Gaussian exponent of 1.0. Vibrational frequencies were evaluated at the SCF level using analytic second derivative methods<sup>10</sup>. The TZP basis was extended to  $[5s\ 3p\ 2d]/[3s\ 2p]$  for use in MP2 calculations: an additional

$d$  set was added (a two-term fit to a Slater function with exponent 0.7), while the original hydrogen  $p$  set was replaced by two functions with Gaussian exponents 1.4 and 0.35. Finally, in the largest of these MP2 calculations the  $[5s\ 3p\ 2d]/[3s\ 2p]$  basis was augmented with an  $f$  set (exponent 1.9) on each of the fluorine atoms. All of these initial SCF and MP2 calculations utilized the program GRADSCF.<sup>11</sup>

For more elaborate studies of correlation effects, an atomic natural orbital (ANO) basis<sup>12</sup> of the form  $[4s\ 3p\ 2d\ 1f/3s\ 2p\ 1d]$  was used. This was contracted from a  $(13s\ 8p\ 6d\ 4f/8s\ 6p\ 4d)$  primitive set: the fluorine  $s$  and  $p$  exponents and the hydrogen  $s$  exponents are taken from van Duijneveldt<sup>13</sup> and the polarization functions are even-tempered expansions  $\alpha\beta^k$ ,  $0 \leq k \leq n$ . The ratio  $\beta$  is 2.5 in all cases, with  $\alpha(d) = 0.16$  and  $\alpha(f) = 0.49$  on fluorine and  $\alpha(p) = 0.1$  and  $\alpha(d) = 0.26$  on hydrogen. The ANOs for fluorine were obtained from a single and double excitation CI (CISD) calculation on the atomic ground state, while those for hydrogen were obtained from a calculation on the molecule  $H_2$ .<sup>12</sup>

The first set of infinite-order correlated calculations was performed using the CISD method, including also Davidson's correction for higher excitations<sup>14</sup>, denoted CISD+Q. The second method used was the coupled-pair functional (CPF) method of Ahlrichs and coworkers<sup>15</sup> which is nearly size-extensive. Finally, the coupled cluster method with single and double excitations (CCSD) was used — this is exactly size extensive<sup>16</sup> — together with the method denoted CCSD(T) in which a perturbational estimate of the effect of connected triple excitations is included.<sup>17</sup> In the correlated calculations SCF orbitals were used, and either 24 or 18 electrons were correlated: the former corresponds to neglecting fluorine  $1s$  electron correlation while in the latter correlation is neglected for both fluorine  $1s$  and  $2s$ . No virtual orbitals were deleted in any calculations, and in the ANO basis calculations only the spherical harmonic components of the basis functions were used. The CISD and CPF calculations were performed using the MOLECULE-SWEDEN suite of programs<sup>18</sup>, while the coupled-cluster calculations were performed using the program VCCSD<sup>19</sup>.

## Results and Discussion

### Geometry

Our optimized SCF bond distance in HF is 0.902 Å, compared to an experimental<sup>20</sup> value of 0.917 Å. In the calculated equilibrium structure for the trimer, the H-F bond increases slightly, to 0.910 Å, and the hydrogen-bonded H-F distance is 1.917 Å. Our calculated results are similar to those of Gaw and co-workers<sup>4</sup>, who found  $r(H-F)$  to be 0.912 Å in the monomer and 0.923 Å in the  $C_{3h}$  trimer. Their value for the H-F hydrogen bond distance is 1.860 Å, somewhat shorter than our value, which was determined using

a larger basis set. Our calculated H-F bond distance in the symmetric  $D_{3h}$  trimer is 1.136 Å, in excellent agreement with the value of 1.139 Å found by Gaw *et al.* As we noted above, Karpfen<sup>8</sup>, has included correlation at the ACPF level using a split-valence plus polarization basis set. His optimum bond lengths are 0.919 Å in the monomer and 0.932 Å in the trimer. Correlation thus appears to have a rather small effect on the geometries, although the effect is larger on the trimer than on the monomer.

#### Vibrations:

For HF we calculate a harmonic frequency of 4455  $\text{cm}^{-1}$  with an infrared intensity of 172 km/mol using the TZP basis set at the SCF level. The experimental value is 4138  $\text{cm}^{-1}$ , while Gaw *et al.* calculated a value of 4440  $\text{cm}^{-1}$ , and Karpfen<sup>8</sup>, a value of 4182  $\text{cm}^{-1}$  at the ACPF level. There is a strong dependence of the calculated vibrational frequency on the HF bond length: if the bond is elongated the computed "frequency" decreases sharply. The calculated trimer frequencies are given in Table I.

The hydrogen-bonded systems  $(\text{HF})_n$  have been extensively investigated experimentally. Some of these studies have included investigations of the higher species, although most have focused primarily on the dimer. Klemperer and coworkers<sup>21</sup> have shown that the trimer of HF is non-polar, consistent with a  $C_{3h}$  symmetry structure. Molecular beam predissociation experiments on the trimer have also been performed<sup>22,23</sup>, as have infrared vibrational spectroscopy experiments in neon and argon matrices<sup>24,25</sup>. The vibrational predissociation spectrum of the trimer indicates that the  $e'$  band lies at 3712  $\text{cm}^{-1}$ . Only one of the bands observed in matrix isolation spectra is consistent with a  $C_{3h}$  symmetry structure, the others are presumably due to open-chain forms that may be present in these experiments. This band is found at 3706  $\text{cm}^{-1}$  in a neon matrix, and at 3702  $\text{cm}^{-1}$  in an argon matrix.

Our  $C_{3h}$  structure is a minimum, based on the computed force constants. Of the twelve possible vibrational bands in this molecule there are three infrared active degenerate  $e'$  bands and one infrared active  $a''$  band. Two of these bands, one of  $a'$  and the other of  $e'$  symmetry, correlate with the separated HF molecule fragment vibrations, while the remaining bands in the trimer correlate with translations and rotations in the separated fragments, that is to "intermolecular" modes in the trimer. The symmetric HF stretch is red shifted by 241  $\text{cm}^{-1}$  while the degenerate HF stretch is red shifted by 175  $\text{cm}^{-1}$  from the monomer. The red shift is consistent with the increase in the HF bond distance on going from monomer to trimer, although other factors also play a role, of course. Similar red shifts were computed by Karpfen. Our calculated frequencies are somewhat larger than those of Gaw and coworkers. The intensity of the degenerate  $e'$  stretch is predicted to be very large both in our calculations and in the other studies.

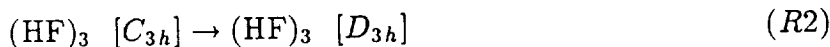
The remaining harmonic frequencies are all below  $1000\text{ cm}^{-1}$  and are associated with the intermolecular librational motions. The symmetric and degenerate hydrogen bond bends are at  $879$  and  $531\text{ cm}^{-1}$ , respectively. The degenerate hydrogen bond bend is predicted to be very intense as is the out-of-plane motion of  $a''$  symmetry.

In order to compare our computed trimer frequencies with experiment, we scale them by a factor of  $0.93$ , which is the ratio of the experimental harmonic frequency of HF monomer to our computed value. Our scaled calculations thus predict a harmonic frequency of  $3919\text{ cm}^{-1}$  for the symmetric H-F stretch and  $3980\text{ cm}^{-1}$  for the degenerate H-F stretch. The experimental <sup>23</sup>, gas phase result is  $3712\text{ cm}^{-1}$  differing from our scaled result by almost  $270\text{ cm}^{-1}$ , and suggesting a remarkably large anharmonicity for this mode. The assignment of the remaining bands appears to be in much better agreement with the available experimental data. We assign the band at  $590\text{ cm}^{-1}$  to the  $a''$  out of plane mode, calculated value of  $596\text{ cm}^{-1}$ , while the band at  $477\text{ cm}^{-1}$  is assigned as the degenerate bend in the  $C_{3h}$  trimer, calculated value  $478\text{ cm}^{-1}$ . Both of these modes are predicted to be intense, while the lowest lying  $e'$  band is calculated to be very weak when compared to the other transitions.

Force constant calculations confirm that the  $D_{3h}$  symmetry structure is a transition state with the direction of negative curvature appropriate for the simultaneous exchange of hydrogens among the fluorines. The magnitude of the imaginary frequency is found to be  $2224i\text{ cm}^{-1}$ , consistent with the dominant motion involving hydrogens. The totally symmetric stretch is about half of its value when compared to the  $C_{3h}$  symmetry trimer. One of the degenerate stretches is much lower ( $1674\text{ cm}^{-1}$ ) than the value found in the  $C_{3h}$  symmetry trimer ( $4280\text{ cm}^{-1}$ ), and one is much higher,  $1506\text{ cm}^{-1}$  versus  $531\text{ cm}^{-1}$ .

#### *Energetics:*

Our discussion of the energetics of the concerted hydrogen exchange is based on the three reactions  $R1$ – $R3$  given in the Introduction: we repeat them here for convenience.



Although ultimately the enthalpy changes are important chemically, we will first focus only on the electronic energy differences. Our results are summarized in Table II, where we present values for each of the three reactions given above with SCF, perturbation theory, CI, as well as the coupled-cluster methods. Our most accurate results suggest that the stable hydrogen bonded trimer is bound by slightly more than  $14\text{ kcal/mol}$  relative to the



separated fragments, the barrier to reaction (*R3*) is predicted to be only 3.6 kcal/mol, and the energy separation between the transition state, and the stable trimer (*R2*) is 18 kcal/mol. This is in marked contrast to the results of most of the previous work cited in the introduction. There is also a substantial variation in the results depending on the correlation treatment employed, as we now discuss.

At the CISD+Q level of correlation treatment, the energy difference between three separated HF molecules and the transition state is found to be small: about 7 kcal/mol. A comparison of this reaction with the covalent exchange of hydrogens in the  $H_6$  system indicates that introduction of ionic character into the molecular system by replacement of three hydrogens with three fluorine atoms reduces the effective barrier from some 70 kcal/mol to about 7 kcal/mol. An approximate quantitative measure of these changes can also be seen by an examination of the Mulliken charges calculated for the trimer and the transition state. At equilibrium the charge on hydrogen is found to be  $0.3e^-$ , whereas at the transition state this increases to  $0.4e^-$ .

As expected, the formation of the  $C_{3h}$  trimer from three monomers is found to be exothermic. The SCF value is found to be 12.4 kcal/mol while each of the correlated treatments predict that the complex is slightly more than 14 kcal/mol more stable than the reactants. The effect of correlation is found to be about 1.7 kcal/mol and roughly independent of the number of electrons correlated or the level of treatment. Liu and coworkers<sup>7</sup> have found that correlation contributed about 1 kcal/mol to this energy, somewhat less than we do. Their value was obtained with a TZP basis, while correlation effects were included at the ACCD level<sup>26</sup>. Karpfen obtains a somewhat larger binding energy (15.4 kcal/mol) at the ACPF level, with a rather small basis. We note, however, that consideration of basis set superposition error changes these observations, as we discuss in detail below.

The effect of correlation is most dramatically seen on the energy difference between the stable complex and the transition state. At the SCF level we find this energy difference to be over 35 kcal/mol, while the simplest correlation treatment (MP2) reduces this energy difference to 16 kcal/mol. More elaborate single and double excitation correlation treatments result in a difference of about 20 kcal/mol. The results are largely insensitive to whether 18 or 24 electrons are correlated, so it would not be unreasonable here to regard the fluorine 2s electrons to be part of an atomic core. On the other hand, there are significant differences between the CISD results and those of the various size-extensive or approximately size-extensive treatments; with such a large number of electrons correlated this would be expected. Thus the simplest CI treatment, CISD, predicts an energy separation of 23.9 kcal/mol, whereas inclusion of the +Q correction reduces this value to

21.1 kcal/mol. CPF reduces this separation by another 1.1 kcal/mol, but this appears to be an overestimate when compared to the CCSD result of 20.9 kcal/mol. Finally, inclusion of the (T) correction for the effects of connected triple excitations reduces the energy separation by almost 3 kcal/mol. This large triples contribution to the barrier height for hydrogen exchange deserves further comment.

On initial examination, such a large effect of triples is unexpected, and might be assumed to indicate that nondynamical correlation (near-degeneracy effects) might be important at the transition state. Recently, Lee et al.<sup>27</sup> have proposed the use of a diagnostic for the effects of nondynamical correlation, based on the magnitude of the norm of the  $t_1$  amplitudes, denoted  $T_1$ . This  $T_1$  diagnostic has been shown to be a good indicator of the applicability of a single-reference-based coupled-cluster method. It was suggested<sup>27</sup> that a value larger than 0.02 for  $T_1$  indicates nondynamical correlation effects are large enough to cast doubt on the reliability of single-reference treatments limited to single and double excitations. For the  $D_{3h}$  geometry of (HF)<sub>3</sub>  $T_1$  is 0.01, which would indicate that nondynamical correlation effects should not be a problem. The large triples contribution in fact arises from a different (and in some respects a simpler) cause. At the transition state we have three chemical bonds which are significantly elongated relative to their equilibrium value. We can examine the effect of triple excitations on this bond-lengthening by computing the triples contribution for a single HF moiety, at equilibrium bond length and at the bond length obtained for the transition state. The triples contribution to the energy difference between these two geometries was found to be a little less than 0.7 kcal/mol. Thus of the 2.9 kcal/mol triples correction to the barrier height, almost 2.1 kcal/mol originates in the simultaneous stretching of three HF bonds. Hence only 0.8 kcal/mol should be ascribed to a true "many-body" effect. Nevertheless, it is clear that in a system where even more bonds participate in the rearrangement, such as hydrogen exchange among higher oligomers of HF, such cumulative effects would be further magnified and would certainly require an appropriate correlation treatment.

We can now examine several sources of error in these calculations. The first is the use of SCF geometries in the correlation treatment. In order to address this question we have reoptimized the structure of the  $D_{3h}$  transition state at the MP2 level using the TZ2P basis augmented by a set of  $f$ -type functions on each of the fluorine atoms. The bond lengths increase slightly (less than 0.01 Å), while the energy is lowered by less than 0.8 kcal/mol relative to the MP2 result at the SCF geometry. Although we have performed only the easier task of reoptimizing the geometry of the  $D_{3h}$  symmetry structure with its two degrees of freedom, we expect the effects of electron correlation to be substantially less for the equilibrium structure than for the transition state, as discussed below. We are therefore confident that our choice of SCF geometries will not be a source of significant

error.

A quantitative assessment of our energetics must include an estimate of the basis set superposition error (BSSE). Ideally, this should be done for both the stable complex and the transition state. However, estimating the BSSE for polyatomic systems like  $(\text{HF})_3$  presents some conceptual difficulties. We have chosen to proceed by computing a counterpoise correction for the stable complex, using the SCF-optimized geometry and with both a single HF molecule with two HF ghost basis sets present and two HF molecules with a single ghost basis present as the fragments. The ANO basis was used in all BSSE investigations. At the SCF level the BSSE is less than 0.1 kcal/mol. However, at the CCSD level the BSSE is slightly greater than 0.5 kcal/mol for *each* HF moiety. We would thus assign a BSSE of 1.5 kcal/mol for the hydrogen-bonded trimer: this is likely to be an overestimate rather than an underestimate. Nevertheless, these results suggest that the effects of correlation on the binding of the trimer are grossly exaggerated, since most of the energy lowering is due to BSSE. This is consistent with the results of Karpfen, who (assuming an SCF result similar to ours) would obtain an even greater correlation contribution to binding: the split-valence plus polarization basis of Ref. 8 is likely to have a larger BSSE than our ANO basis. On the other hand, the results of Liu and co-workers are less consistent with this picture. Finally, the structure of the transition state is not qualitatively different from that of the stable complex, so we can reasonably assign the same (upper bound) value of 1.5 kcal/mol to the BSSE in the transition state.

The incompleteness of the one-particle space is also a source of error in these calculations. Comparison of the MP2 results, at least, in the TZ2P and ANO basis sets, suggests that the effect of basis set extension on the binding energy of the trimer is relatively small. Nevertheless, it is now well understood that the dominant contribution to hydrogen bonding is electrostatic, and so the basis set used should not only correctly describe the bonding in the monomer, but also provide a reasonable description of the multipole moments and polarizability. ANO basis sets are not always capable of meeting these requirements without further augmentation<sup>28</sup>, which would make the present calculations too expensive. It is thus possible that the effect of basis set incompleteness on the binding energy is somewhat underestimated by our calculations. However, it seems unlikely that the remaining effects would contribute more than 1 kcal/mol. Since the bonding in the transition state is similar to that in the stable complex, we expect that the basis set effect on the barrier height would, if anything, be even smaller.

### *Enthalpy Changes*

Our calculated  $\Delta E$  values refer to the bottom of the potential energy well and need to be corrected by the difference in zero point vibrational energy,  $\Delta \text{ZPE}$ . Our correction

is done at the harmonic level using the experimental value for the HF frequency, while the trimer values are derived from our calculated frequencies scaled by 0.93 as indicated above. The stable trimer contains 4.5 kcal/mol more vibrational energy than the separated reactants which reduces its stability to 9.9 kcal/mol. Correcting this value for BSSE will further reduce the stability of the trimer: if the full counterpoise correction is applied the result would be as low as 8 kcal/mol. In view of our discussion of basis set incompleteness, it seems reasonable to assert that the trimer is bound by  $9 \pm 1$  kcal/mol.

The  $\Delta ZPE$  correction between the transition state and stable trimer is  $-3.5$  kcal/mol, while it is  $1.1$  kcal/mol between the transition state and the reactants. Given these values our calculated barrier at 0 K is  $4.7$  kcal/mol, and the energy separation between the stable trimer and the transition state is  $14.5$  kcal/mol. Each of these values may then be further corrected for BSSE, which would raise the computed barrier to  $6.2$  kcal/mol.

These results require further correction for non-zero temperatures. For reaction R2 there are no corrections required to convert  $\Delta E$  to  $\Delta H$  if we neglect the dependence of the vibrational energy on temperature. For R1 and R3 the values must be corrected for differences in the translational and rotational energies and for the difference between  $\Delta E$  and  $\Delta H$  ( $\Delta H = \Delta E + \Delta n RT$  with  $\Delta n = -2$ ). The correction term is  $-6.5 RT$  and at 300 K this corresponds to a value of  $-3.9$  kcal/mol for the correction, or a barrier of  $2.3$  kcal/mol, if the BSSE value for the barrier is used.

## Conclusions

We have investigated the exchange of hydrogen atoms in a hydrogen-bonded system and have shown that such an exchange can proceed with an activation energy of  $\approx 4$  kcal/mol. In addressing this problem we have also demonstrated that the presence of ionic character in the bonding lowers the barrier relative to that found in a purely covalent system, such as  $H_6$ . The effects of electron correlation on the energetics once again demonstrate the magnitude of size-extensivity errors when many electrons are correlated. In addition, in  $(HF)_3$  the effects of triple excitations significantly alter the barrier height from that predicted at the CCSD level, and we can expect this effect to become more important with increasing size of the system. Finally, since the barrier to concerted hydrogen exchange is small, we may anticipate a significant contribution from tunneling to the rate of the exchange reaction.

## Acknowledgement

We would like to gratefully acknowledge the support by Cray Research, Inc. in providing one of us (AK) with time on their computers, without which much of this work would not have been possible.

## References

1. P. R. Taylor, A. Komornicki and D. A. Dixon, J. Am. Chem. Soc. **111**, 1259 (1989)
2. D.A. Dixon, R.M. Stevens, D.R. Herschbach,  
Faraday Disc. Chem. Soc. **62**, 110 (1977)  
J.S. Wright Chem. Phys. Lett. **6**, 476 (1970)  
J.S. Wright Can. J. Chem. **53**, 549 (1975)
3. D.R. Herschbach, Faraday Disc. Chem. Soc. **55**, 233 (1973)
4. J.F. Gaw, Y. Yamaguchi, M.A. Vincent and H.F. Schaefer III,  
J. Am. Chem. Soc. **106**, 3133 (1984)
5. D. Heidrich, M. Ruckert, H.-J. Kohler, Chem. Phys. Lett. **136**, 13 (1987)  
D. Heidrich, H.-J. Kohler, D. Volkmann, Int. J. Quantum Chem. **27**, 781 (1985)
6. A. Karpfen, A. Beyer, and P. Schuster, Chem. Phys. Lett. **102**, 289 (1983)
7. S. Liu, D.W. Michael, C.E. Dykstra, and J.M. Lisy, J. Chem. Phys. **84**, 5032 (1986)
8. A. Karpfen, Inter. J. Quantum Chem. Symp. **24**, 129 (1990)
9. T.H. Dunning Jr., J. Chem. Phys. **55**, 716 (1971)
10. H.F. King and A. Komornicki in *Geometrical Derivatives of Energy Surfaces and Molecular Properties*, ed. P. Jorgenson and J. Simons, NATO ASI series C. Vol 166. D. Reidel, Dordrecht 1986.  
H.F. King and A. Komornicki, J. Chem. Phys. **84**, 5645 (1986)
11. GRADSCF is an *ab-initio* gradient program system designed and written by A. Komornicki at Polyatomics Research Institute.
12. J. Almlof and P.R. Taylor, J. Chem. Phys. **86**, 4070 (1987)
13. F.B. van Duijneveldt, IBM Res. Report RJ945 (1971)
14. S.R. Langhoff and E.R. Davidson  
Int. J. Quantum Chem. **8**, 61 (1974)
15. R. Ahlrichs, P. Scharf and C. Erhardt, J. Chem. Phys. **82**, 890 (1985)
16. S.A. Kucharski and R.J. Bartlett, Adv. Quantum Chem. **18**, 281 (1986)  
R.J. Bartlett, J. Phys. Chem. **93**, 1697 (1989)

17. K. Raghavachari, G.W. Trucks, J.A. Pople and M. Head-Gordon,  
Chem. Phys. Lett. **157**, 479 (1989)
18. MOLECULE-SWEDEN is a vectorized electronic structure suite of programs written  
by J. Almlöf, C.W. Bauschlicher, Jr., M.R.A. Blomberg, D.P. Chong, A. Heiberg,  
S.R. Langhoff, P.A. Malmqvist, A.P. Rendell, B.O. Roos, P.E.M. Siegbahn, and P.R.  
Taylor.
19. T.J. Lee and J.E. Rice, Chem. Phys. Lett. **150**, 406 (1988)
20. K.P. Huber, G. Herzberg, "*Constants of Diatomic Molecules*", (Van Nostrand, Rein-  
hold, New York, 1979)
21. T.R. Dyke, B.J. Howard and W.J. Klemperer, J. Chem. Phys. **56**, 2442 (1972)
22. J.M. Lisy, A. Tramer, M.F. Vernon and Y.T. Lee, J. Chem. Phys. **75**, 4733 (1981)
23. J.M. Lisy and D.W. Michael J. Chem. Phys. **85**, 2528 (1986)
24. L. Andrews, V.E. Bondybey, J.H. English, J. Chem. Phys. **81**, 3452 (1983)
25. L. Andrews, G.L. Johnson, J. Phys. Chem., **88**, 425 (1984)
26. K. Jankowski, J. Paldus, Int. J. Quantum Chem. **18**, 1243 (1980)  
R.A. Chiles, C.E. Dykstra, Chem. Phys. Lett. **80**, 69 (1981)  
S.M. Bachrach, R.A. Chiles, and C.E. Dykstra, J. Chem. Phys., **75**, 2270 (1981)
27. T.J. Lee, J.E. Rice, G.E. Scuseria and H.F. Schaefer III,  
Theor. Chim. Acta **75**, 81 (1989)  
T.J. Lee and P.R. Taylor, Int. J. Quantum Chem. Symp. **23**, 199 (1989)
28. J. Almlöf and P.R. Taylor, Adv. Quantum Chem. In press.

**Table I**  
**Calculated harmonic vibrational spectra**

Mode	$\omega$ (cm <sup>-1</sup> )	I(km/mol)	Description
<i>C</i> <sub>3h</sub> Structure:			
<i>a'</i>	4214	0	symmetric HF stretch
<i>a'</i>	879	0	symmetric bend
<i>a'</i>	186	0	symmetric stretch -libration
<i>a''</i>	662	507	out of plane torsion
<i>e'</i>	4280	571	degenerate HF stretch
<i>e'</i>	531	382	degenerate angular def.
<i>e'</i>	157	17	degenerate stretch - libration
<i>e''</i>	475	0	degenerate out of plane torsion
<i>D</i> <sub>3h</sub> Structure:			
<i>a'</i> <sub>1</sub>	2212	0	symmetric breathing stretch
<i>a'</i> <sub>1</sub>	788	0	symmetric HF str. and bend
<i>a'</i> <sub>2</sub>	2194 <i>i</i>	–	negative curvature stretch
<i>a''</i> <sub>2</sub>	1449	466	out of plane torsion
<i>e'</i>	1674	21	degenerate stretch plus bend
<i>e'</i>	1506	4154	degenerate stretch + bend
<i>e'</i>	604	0.3	degenerate bend + stretch
<i>e''</i>	1135	0	degenerate out of plane torsion

**Table II**  
**Comparison of relative energies<sup>a</sup>**

Calculation:	$\Delta E(R1)$	$\Delta E(R2)$	$\Delta E(R3)$
SCF, CI, and CPF Results:			
ANO SCF	-12.4	35.8	23.4
ANO CISD 18 el	-14.2	23.8	9.6
ANO CISD+Q 18 el	-14.1	21.3	7.2
ANO CPF 18 el	-14.1	20.8	6.7
ANO CISD 24 el	-14.3	23.9	9.6
ANO CISD+Q 24 el	-14.2	21.1	6.9
ANO CPF 24 el	-14.1	20.0	5.9
SCF, MP2, and CC Results:			
TZ2P/SCF		35.1	
TZ2P/MP2		16.7	
ANO SCF	-12.4	35.8	23.4
ANO/MP2	-14.3	16.1	1.8
ANO CCSD 24 el	-13.9	20.9	7.0
ANO CCSD(T) 24 el	-14.4	18.0	3.6

a) Relative energies are given in kcal/mol.